LAWRENCE
LIVERMORE
NATIONAL
LABORATORY

LLNL-JRNL-464385

# High-Power Solid-State Lasers from a Laser Glass Perspective

J. H. Campbell, J. S. Hayden, A. J. Marker

December 22, 2010

Internationakl Journal of Applied Glass Science

## Disclaimer

# High-Power Solid-State Lasers from a Laser Glass Perspective

John H. Campbell, Lawrence Livermore National Laboratory, Livermore, CA

Joseph S. Hayden and Alex Marker, Schott North America, Inc., Duryea, PA

## Abstract

Advances in laser glass compositions and manufacturing have enabled a new class of high-energy/high-power (HEHP), petawatt (PW) and high-average-power (HAP) laser systems that are being used for fusion energy ignition demonstration, fundamental physics research and materials processing, respectively. The requirements for these three laser systems are different necessitating different glasses or groups of glasses. The manufacturing technology is now mature for melting, annealing, fabricating and finishing of laser glasses for all three applications. The laser glass properties of major importance for HEHP, PW and HAP applications are briefly reviewed and the compositions and properties of the most widely used commercial laser glasses summarized. Proposed advances in these three laser systems will require new glasses and new melting methods which are briefly discussed. The challenges presented by these laser systems will likely dominate the field of laser glass development over the next several decades.

## I. Introduction

This year (2011) marks the fiftieth anniversary of Snitzer's first glass laser [1]. This discovery is chronicled in his owns words in a remarkable personal interview published by the American Institute of Physics [2]. Few are aware that Snitzer's great invention came on the heels of unjust accusations and treatment by the infamous 1950's U.S. House of Representatives Committee on Un-American Activities. Snitzer's work during that time proved he is not only a great scientist but also a man of principle and tremendous courage.

This work was performed under the auspices of the U.S. Department of Energy by Lawrence Livermore National Laboratory in part under Contract W-7405-Eng-48 and in part under Contract DE-AC52-07NA27344.

Snitzer's discovery spawned many new inventions in the field of lasers, optical devices and fiber communications. In this manuscript we focus on just one of these areas: glass lasers for high-power applications and the laser glasses (gain media) that comprise the heart of these lasers.

We begin with a generic description of a laser and then explain the Nd-doped glass laser and its operation in conceptual terms. Our description is not meant to supplant the many outstanding texts on lasers (see for example [3-6]). Instead the goal is to provide a common starting point for the readers of this journal who may be unfamiliar with certain aspects of laser design and operation. Interested readers should particularly consult references 3 and 6; these sources focus on solid state lasers with significant treatment of glass lasers.

Next, we briefly describe the three main types of high-power glass lasers that are currently operational. Also included is a description of the laser glasses used in each of the three systems. This is followed by a summary of key laser glass properties and composition space important for high-power applications. A short description of the glass manufacturing methods available to meet current and near term requirements is also presented.

One is lead to the conclusion that after 50 years of glass laser development, the suite of glasses suitable for use in high power laser glass systems is surprisingly small. The reasons for this are discussed.

A case is made that developing new glasses with much improved thermal mechanical properties, while maintaining good laser and optical properties, will be the biggest challenge for meeting the needs of the next generation of high power glass lasers. Examples of promising glasses and the required manufacturing methods are discussed. Competition from single-crystals and transparent polycrystalline ceramics offer a potential replacement for laser glasses, but face significant challenges in achieving the quality, size and throughput that are the hallmarks of optical glass melting.

## II. Glass lasers: an overview

In its simplest configuration a laser consists of a gain-media positioned inside a resonate cavity (Fig 1a). The gain-media is the photon generator; it can be a solid, liquid, gas or plasma. Energy is stored in

the gain media by means of "pumping" using an external energy source. The pump energy induces transitions in atoms or molecules from lower to higher energy levels (rotational, vibrational and/or electronic) and, under proper conditions, one achieves the necessary population inversion between two energy levels required for laser action.

The resonant cavity that contains the gain medium is comprised of a high reflectivity mirror on one end and a partially reflective mirror ("output coupler"), on the other. The output coupler functions as the name implies, it transmits a fraction of the light circulating in the resonator cavity into an output beam. If the output coupler operates in a steady-state mode (constant energy output) it is termed "continuous wave" laser operation. In contrast, some output couplers are designed to abruptly change from near 0% transmission to 100%. This configuration allows one to dump all or part of the energy circulating in the resonator into a single pulse, hence the term pulse-mode operation. The high-power glass lasers that are the focus of this article operate in the pulsed-mode.

The system comprised of the resonator cavity, gain medium and pump source is commonly called a laser "oscillator". A variant of the simple oscillator design, of importance for the discussions here, is shown in Fig 1b. Here the output from the oscillator is directed to a second pumped gain medium that functions as an amplifier. There are many advantages to the oscillator/amplifier concept, chief being the ability to generate high energy/high power laser outputs. For example it is straight forward to imagine laser designs employing multiple amplifiers and/or multi-pass amplifier configurations to generate high power output. Such design concepts form the basis for the high-energy/high-power glass lasers in operation today.

Glass lasers are a sub-set of solid-state lasers where the gain medium consists of rods or plates (slabs) of optical quality glass doped with a lasant ion [3,6]. A common dopant ion, and the one used by Snitzer in his original laser, is $Nd^{3+}$. Typically, $Nd^{3+}$-doped laser glass plates or rods are installed in a flashlamp-pumped cavity as shown schematically in Fig 2. When the laser is "fired", a capacitor bank sends an electrical discharge through a xenon-containing flashlamp that in turn produces an intense pulse of white-light with a spectral distribution that overlaps the absorption bands of the $Nd^{3+}$.

The pumping and amplification process by the Nd-laser glass can be described in terms of either an engineering or atomistic representation as shown in Fig 3. In the simpler "engineering" representation (Fig. 3a) the laser glass stores optical energy delivered by the flashlamps. The stored energy in the glass is characterized by a gain coefficient, g. As a weak input pulse (i.e. small signal) propagates through the glass, the pulse energy increases exponentially with the distance, L (cm), as given by [5]:

$$I_{out} / I_{in} = \exp (g L) \quad (1)$$

where $I_{in}$ and $I_{out}$ are the pulse input and output intensity ($W/m^2$), respectively. The small-signal gain, $G_o$, of the system is defined as the ratio of the output to input intensity:

$$G_o = I_{out} / I_{in.} \quad (2)$$

It is important to recognize the distinction between the gain coefficient, which is a material property, and the gain, which is a system performance measure. The unfortunate choice of wording often leads to confusion in the use of these two terms.

In the more fundamental "atomistic" representation (Fig 3b), the flashlamp light excites ("pumps") the Nd $^{3+}$ 4f electrons from the ground state ($^4I_{9/2}$) to a manifold of higher energy states. The electrons rapidly relax to the meta-stable $^4F_{3/2}$ state by a series of non-radiative energy transitions to glass phonon modes (heat). The non-radiative loss rate is slow between the meta-stable $^4F_{3/2}$ level and the lower lying $^4I$ states because of the large energy gap between them. This leads to an accumulation of electrons at this level and generates the population inversion necessary for laser action. A weak laser pulse, with a wavelength matched to the energy between the $^4F_{3/2}$ and $^4I_{11/2}$ states, stimulates the transition between these two states and coherently adds energy to (amplifies) the transmitted pulse. The electrons in the terminal laser level ($^4I_{11/2}$) rapidly relax to the ground state. Note that $Nd^{3+}$ is an example of a "four level" laser system [3,7]: (1.) ground state -$^4I_{9/2}$ (2.) the manifold of pump bands (3.) upper laser level - $^4F_{3/2}$ and (4.) terminal laser level - $^4I_{11/2}$.

The atomistic representation allows one to express the gain coefficient (g) in terms of more fundamental properties of the $Nd^{3+}$ glass system:

$$g = [\sigma(\lambda)N^* - \alpha] \quad (3)$$

where $\sigma(\lambda)$ is the $Nd^{3+}$ emission cross-section ($cm^2$) at wavelength $\lambda$, N* the $Nd^{3+}$ inversion density at the $^4F_{3/2}$ state ($1/cm^3$) and $\alpha$ the absorption coefficient ($cm^{-1}$) at the laser wavelength. The emission cross-section is a measureable quantity and physically represents the effective interaction area of $Nd^{3+}$ in the $^4F_{3/2}$ state with a propagating photon of wavelength ($\lambda$). Consequently, the greater the cross-section the more likely the interaction and the greater the gain achieved.

Note from Eq. 3 that the gain coefficient is comprised of two terms. The first term ($\sigma(\lambda)N^*$) describes the amplification due to the stimulated emission from the upper laser level whereas the second defines the energy loss due to absorption ($\alpha$) by impurities in the glass. Therefore, to achieve a large gain requires a glass composition for which the $Nd^{3+}$ emission cross-section is maximized, combined with efficient optical pumping to achieve a large population inversion (N*). In addition, the glass must be manufactured with high purity to minimize transmission losses due to absorbing impurity ions.

It is instructive to compare the magnitude of various terms in Eq. 3 for a typical flashlamp-pumped amplifier; for example, consider a high-power laser amplifier used on a fusion energy research laser (these lasers are described in the next section). A typical amplifier small-signal gain coefficient has a value of about 0.05 $cm^{-1}$. In other words, the weak laser pulse is amplified exponentially by 5% for every cm of glass it propagates through. The absorption loss ($\alpha$) of the laser glass is also measured during manufacture and is typically <0.001 $cm^{-1}$; thus the loss is less than $1/50^{th}$ of the gain.

The measured $Nd^{3+}$ emission cross-section for the glasses used in these lasers is about $4\times10^{-20}$ $cm^2$ [8] and can be used to estimate the excited-state density in the meta-stable state from the gain coefficient (i.e. $N^*=g/\sigma$). N* is computed to be approximately $1.3\times10^{18}$ $/cm^3$ based on a value of $0.05cm^{-1}$ for g. The excited state density, N*, has greater physical meaning when expressed in terms of the "stored energy" in the glass. Recall that each electron in the meta-stable state can potentially produce a stimulated laser photon of energy, $h\nu$ ($1.885\times10^{-19}$J), and the product $N^*h\nu$ is the optical energy stored in the glass that could be extracted during a laser shot. The stored energy in the laser glass is about 250 J/liter for this example. The amount of the stored energy that is extracted by the incident laser pulse depends on a

number of factors (laser design, pulse intensity, pulse length, etc) and can range from less than a few percent to as much as 80%.

The Nd-doped laser glasses used in high power systems are predominantly phosphate based with near meta-phosphate compositions. The reasons for this choice are described in more detail later but, in brief, Nd-phosphate glasses present the following main advantages:

- Large stored energy
- Efficient energy extraction
- Resistance to laser-induced damage
- Mature manufacturing technology

The choice of which specific phosphate glass to use depends on the type of glass laser. In the next section the three main classes of high-power glass lasers and their primary applications are described. This provides the launching point for the subsequent discussion of laser glass properties and compositions.

## III. Current high power glass lasers

In general, current high power glass lasers can be divided into three broad classes as given in Table 1. HEHP and PW laser systems are essentially single-shot devices designed to be fired and then allowed to cool several hours before re-firing. In contrast, the HAP lasers are designed to operate continuously at repetition rates typically in the range of ~1-10 Hz.

### A. HEHP Lasers for Inertial Fusion Research

HEHP glass lasers are predominantly used for Inertial Confinement Fusion (ICF) research [9,10]. There are currently multi-kilojoule HEHP glass laser systems in operation around the world (Table 2); the major centers are in Japan [11], China [12, 13], Russia [14], France [15], and the US. Within the US there are three major facilities, all sponsored by the US Department of Energy: the Laboratory for Laser

Energetics at the University of Rochester, LLE [16,17], the Beamlet laser at Sandia National Laboratory [18,19] and the National Ignition Facility (NIF) at Lawrence Livermore National Laboratory, LLNL [20,21].

All major HEHP glass laser systems use Nd-doped phosphate glasses; Table 2 provides the commercial code designation and Table 3 a compilation of key properties for those in most common use. The majority of these glasses originate from two commercial suppliers: Schott [22] and Hoya [23]. Smaller quantities and sizes have also been provided by Kigre Inc. [24] for certain lasers in the US. The glasses for the lasers in China and Russia are manufactured within each country under the code designations N31 and KGSS-0180/35-grade, respectively (Table 3). Brief descriptions of the melting technology and properties of the N31 glass used in China have been published recently [25] and, as stated by the authors, mimic closely the glasses and manufacturing methods developed by Schott and Hoya with LLNL [8,26-31].

The glass property compilation in Table 3 represents the most recently reported values, to the best of our knowledge. Most come from current company marketing data sheets, recent measurements in our own laboratories or from recent literature sources as so noted. Values for some properties may differ slightly (generally <10%) from earlier compilations due to measurement variations between laboratories, improved or new measurement methods and/or small changes in compositions; for example the Nd-doping level can cause small variations in many properties. Also, some laboratories report measurements at slightly different temperatures or over different temperature ranges (e.g. thermal expansion coefficient); these are noted in Table 3, when reported. In any event, the differences are small and should have minor impact for most applications; if needed more information can be obtained by contacting the glass vendor. (This same comment applies to the property compilation of HAP glasses (Table 4) as discussed in the next section.)

One example of a mega-joule scale HEHP laser system is the National Ignition Facility (NIF) that began full-scale operation in 2009 at the Lawrence Livermore National Laboratory (LLNL) [20,21]. The name of the facility is derived from its purpose: to achieve controlled thermonuclear (fusion) ignition in a

laboratory setting [9,10]. The NIF is the largest laser, as well as largest optical system, ever constructed [32] and is capable of irradiating mm-size targets contained in a 10-m diameter target chamber with energies up to 1.8MJ at 351 nm and peak powers of $5.0 \times 10^{14}$ W (500TW) [21,33]. The NIF contains more than 7500 large optics of 40 cm or greater transverse size including laser amplifier glass slabs, lenses, mirrors, polarizers, and crystals and an additional 26,000 smaller optical components (< 20 cm). The total area of precision optical surfaces in NIF is nearly 4,000 $m^2$. The building that houses the laser, beam propagation optics and target chamber covers an area > $10^4$ $m^2$.

The NIF utilizes 192 identical laser beam-lines to achieve its mega-joule output energies [20].The main glass laser amplifiers are grouped in two laser bays each of which contains half (96) of the laser beamlines (Fig 4). Each beam-line contains 16 precision polished, Nd-doped, phosphate glass plates (3072 for the full system) and each plate measures $81 \times 46 \times 4$ $cm^3$. The laser glass plates are installed in a series of cassettes (Fig. 5) that are then installed in flashlamp-pumped amplifiers. When the laser is "fired", a capacitor bank sends a 0.36 ms electrical discharge (60kV and 25 kA) through 7680 xenon-containing flashlamps (each ~2.5m long). The flashlamps generate an intense pulse of white-light (~30kJ/lamp) with a spectral distribution that overlaps the absorption bands of the $Nd^{3+}$ in the laser glass (see Fig 3b). The NIF uses two commercially available laser glasses in the main amplifiers: Schott's LG-770 and Hoya's LHG-8 (Table 3). The glasses have an Nd doping density of $4.2 \times 10^{20}$ $Nd/cm^3$.

B. High average power (HAP) lasers for material processing.

High average power (HAP) glass laser systems are predominantly used for commercial materials processing, particularly laser peening of metals. Laser peening (LP) is a surface treatment process developed to improve fatigue performance and strength of high-value metal parts, particularly those used in aerospace applications. Extensive literature exists on the LP process and two recent sources contain a through compilation of much of this work [34, 35].

To our knowledge, only two companies provide this capability in a commercial setting: Metal Improvement Company Inc. [36] and LSP Technologies Inc. [37]. Each has proprietary HAP laser

systems and peening technology. Both companies use commercial laser glasses specifically formulated for high power applications (Table 4). Metal Improvement Inc. operates in the US and Europe and also fields self-contained mobile laser systems on a semi-trailer that can be transported to the customer's site [36]. The LP beam is then "piped" to the work piece; in principle there is no size limit to the work piece and, if so required, could be a full-size aircraft, a ship or other large structure.

The laser peening process is schematically shown in Fig 6. In brief, the pulsed output from a HAP laser is used to irradiate either the bare metal surface or a thin sacrificial ablation layer that has been applied to the surface. The laser interaction with the part surface causes it to rapidly heat, vaporize and partially ionize, generating a plasma with temperature ~$10^4$ K (~1 eV). The rapid vaporization and expansion of the ablated material is inertially confined by a thin layer of water that flows laminarly over the LP surface and serves as a tamper that intensifies the pulse pressure. The ablation pressure scales as the square-root of the irradiance. Typically an irradiance of 10GW/cm$^2$ (at ~15-20ns pulse width) generates a peak pressure of ~2.5GPa (25 kbar). The pressure pulse launches a shock wave that propagates through the metal. The plastic-deformation of the metal by the shock wave produces a permanent compressive residual stress that penetrates to a depth of between 1 to 8 mm depending on the material and the processing conditions. Multiple firings of the laser in a pre-defined spatial pattern imparts a layer of residual compressive stress over the desired area of the part. The compressive stress layer creates a barrier to crack initiation and growth, which consequently enhances the fatigue life and can provide resistance to stress corrosion cracking and fretting [34, 35].

An example of a HAP glass laser used for laser shock peening has been described by Dane et al [38,39]. The laser employs a "zig-zag" amplifier design (Fig 7) referring to the fact the extraction pulse propagates within the glass in a zig-zag pattern controlled by total-internal-reflection at the slab/water interface. The slab is positioned in the center of the amplifier assembly and has water cooling channels along the sides formed by the slab face and a clear glass window. Flash-lamps located along the slab faces pump the laser glass through the window. The glass is configured in a thin slab shape to enhance the

conductive heat removal from the slab center to the cooling water. Dane et al [39] report slab dimensions of ~1 × 14 × 40 cm with nominal Nd doping levels of ~$3 \times 10^{20}/cm^3$.

C. Petawatt (PW) glass lasers for basic science and advanced fusion research.

Petawatt glass laser development has shown tremendous growth since the demonstration by Perry et. al. of a 1.25 PW ($1.25 \times 10^{15}$ W) Nd-glass laser [40, 41]. This growth has been driven largely by the realization that so-called "table top" PW lasers can been built with modest funds thus making these systems available to university researchers. Petawatt powers provide access to a new regime of laser-matter interactions of interest for fundamental physics studies [42, 43]. In addition, Tabak's proposed "fast ignition" scheme [44] for achieving hot-spot fusion ignition with PW scale lasers has spurred significant interest in the ICF research community.

Forty-five centers for PW laser research are listed in a 2010 compilation provided by the International Committee on Ultra-high Intensity Lasers [45] and include sites in the US, Canada, England, France, Russia, Italy, Germany, Japan, China, India, and South Korea. In general, the Petawatt systems fall into two major categories: (i) large-scale, high-energy systems that are constructed as add-ons to existing multi-kilojoule fusion-research lasers [for example 11, 15, 17, 21] and (ii) smaller scale, lower energy "table-top" lasers built mainly at universities [for example, 42].

To generate petawatt powers requires simultaneously achieving two often conflicting operating conditions: short pulse lengths (femto to pico-seconds) and modest to high energies (>100 J). Either condition by itself is readily accomplished with today's laser technologies. However to achieve both simultaneously requires amplification at short pulse lengths which in turn can lead to unacceptable laser-induced damage to the amplifier gain medium. The damage is a consequence of the intensity dependence of the refractive index of the gain media leading to self-focusing as discussed more in Section IV.

The approach used to conquer this problem is to first generate the required short pulse then temporally "stretch" it to a longer pulse length (i.e. lower intensity) for amplification and finally re-compress it back to the initial pulse length (Fig 8). Many PW laser researchers use laser-pumped

titanium-doped sapphire ($Ti^{3+}$:$Al_2O_3$) to generate the initial short pulse. Ti-sapphire offers high-gain over a broad bandwidth which is essential to short pulse generation. Chirped-pulse amplification (CPA) is then used to stretch, amplify and recompress the pulse. CPA was first successfully demonstrated for solid-state lasers in the late 1980s at the University of Rochester [46] and revolutionized Petawatt laser research.

It was recognized early on that an all-Ti:sapphire laser is inadequate for achieving the necessary PW energy and power output. Instead a hybrid system was developed using a laser-pumped Ti:sapphire oscillator plus pre-amplifier for short pulse generation followed by flashlamp-pumped Nd-doped glass power-amplifiers in the long-pulse section. The short pulse output is typically "stretched" in time by a factor of ~$10^4$ from the few hundred femtosecond to nanosecond range. The resulting weak nanosecond pulse is then amplifed using conventional HEHP glass power-amplifer technology to energies in the range of ~$10^2$ - $10^3$J. Matched sets of grating-pairs are used in the stretcher and compressor sections. In fact, a key optical technology for the success of CPA has been the development of advanced gratings [47]. Futher details of the design of PW CPA systems are beyond the scope of this review; instead the reader is referred to [41,42, 48] and work cited there in.

Laser glasses used in PW systems must meet two somewhat conflicting requirements: broad emission bandwidth and low saturation fluence. PW lasers require gain media with broad spectral bandwidths ($\Delta\nu$) to accommodate the short puse widths [40, 48]. This limitation is generally expressed by the pulse-length ($t_p$) times bandwidth ($\Delta\nu$) product (FWHM), which for a chirped gaussian-shape pulse tis [5,40]:

$$t_p \, \Delta\nu \sim 0.5 \qquad (4)$$

The exact value of the product varies somewhat depending on the pulse shape. [5] Nevertheless, the issue remains the same: laser glasses used to amplify very short temporal pulses must have broad gain (emission) bandwidths.

The glass should also have a low saturation fluence ($F_{sat}$) to effectively amplify the pulse (i.e. extract energy from the glass) without laser damage or wavefront distortion. The saturation fluence is given by:

$$F_{sat} = h\nu/\sigma \quad (5)$$

where $h\nu$ is the energy of the laser photon (J) and $\sigma$ is the emission cross-section of the lasant ion ($cm^2$), in this case $Nd^{3+}$. Physcially a saturation fluence of 1 represents a progating energy density (fluence, $J/cm^2$) equivalent to one laser photon per unit-area equal to the $Nd^{3+}$ emission cross-section. To achieve a low saturation fluence requires a high emission cross-section. The conflict in desired amplifier glass properties arises because the lasant ion cross-section and emission bandwidth are inversely related (see section IV A). Consequently a low saturation fluence represents a small bandwidth and vice versa.

Some PW researchers have turned to using a combination of glasses to achieve the required performance. Hays et al [48] recently proposed a multi-petawatt to exawatt laser based on a clever combination of a suite of Nd:doped glasses with varying cross-sections, bandwidths and peak emission wavelengths. The glasses were selected from an extensive compilation of laser, optical, and physical property data on nearly 250 Nd-doped glass compositions prepared and characterized during the 70s and 80s. Table 5 lists several laser glasses in use on PW systems including the ones proposed by Hays et al.

## IV. Laser glass properties important for high power laser applications

In the previous section we listed the key properties of laser glasses used on today's HEHP, HAP and PW systems in Table 3-5, respectively. However little explanation was given as to why these properties are important; that is the purpose of this section. Our treatment, however, is by no means exhaustive. Typically more than twenty individual glass properties must be optimized or controlled to give the desired laser glass performance and this does not include many of the properties important for manufacturing. Here we examine just a few key properties. Several sources and the reference listed therein provide further details [8, 49-52].

A. Emission cross-section and quantum yield

It can be argued that the two most important laser glass properties for high-power applications are the emission cross-section and quantum yield. These two properties largely control the energy storage, gain coefficient, and extraction efficiency of the laser glass. For high power applications, the general goal is to store and extract as much laser energy as possible.

The $Nd^{3+}$ cross-section is determined from analysis of the absorption and emission spectra (Fig 9). The emission spectrum corresponds to the $^4F_{3/2}$ to $^4I_{11/2}$ transition and usually peaks near 1.05-1.06 μm; this is the dominant $Nd^{3+}$ transition and the one of greatest interest for laser applications. The emission band is characterized in terms of the peak emission wavelength ($\lambda_p$) and the effective bandwidth, $\Delta\lambda_{eff}$ :

$$\Delta\lambda_{eff} = \int I(\lambda)\, d\lambda / I(\lambda_p). \quad (6)$$

There are another three emission bands associated with transitions from the $^4F_{3/2}$ to the other $^4I_J$ states (i.e. $^4I_{7/2,9/2,13/2}$), but they are considerably weaker. The relative strength of each emission band is expressed in terms of the branching ratio, $B_J$, which is defined as the fraction of the total fluorescence that terminates at a particular $^4I_J$ state (J=7/2, 9/2, 11/2 or 15/2) and $\Sigma B_J = 1$.

The absorption spectrum is used to determine the branching ratio and radiative lifetime, $\tau_{rad}$, by an analysis method known as the Judd-Ofelt (J-O) treatment [53,54]. In a classic paper, Krupke [55] provided glass chemists with a road map for use of the J-O treatment to assess key laser glass properties from straight-forward spectroscopic measurements on samples from small-scale test melts. The J-O method is widely used and a number of texts describe the treatment in detail (see for example [7]).

The quantities determined from the spectral analysis and J-O treatment (i.e. $B_{11/2}$, $\lambda_p$, $\tau_{rad}$ and $\Delta\lambda_{eff}$) are used to calculate the emission cross-section using the Einstein relation [5,7]

$$\sigma(\lambda_p) = \lambda_p^4 B_{11/2} / (8\pi c n^2 \tau_{rad} \Delta\lambda_{eff}) \quad (7)$$

where n is the refractive index at $\lambda_p$ and c is light speed (m/s). Cross-sections for several commercial Nd-phosphate laser glasses are listed in Tables 3-5 and usually range from $3\text{-}4 \times 10^{-20}$ $cm^2$

The quantum efficiency ($\varepsilon_{eff}$), sometimes also called the quantum yield, represents the fraction of the excited state density in the upper laser level ($^4F_{3/2}$) that relaxes via radiant emission (fluorescence) and is commonly defined as [7,8]:

$$\varepsilon_{eff} = \tau_{meas} / \tau_{rad} \quad (8)$$

where $\tau_{meas}$ is the measured emission lifetime. In practice the quantum efficiency is never unity due to various non-radiative loss mechanisms that divert some fraction of the available stored energy to heat and measurably shorten the emission lifetime. These non-radiative losses are affected by the intrinsic properties of the laser glass as well as the purity with which the glass is manufactured [56, 57]. Figure 10 presents a schematic representation of the most important $Nd^{3+}$ non-radiative loss mechanisms in phosphate glasses [8, 56]. Impurities with absorption bands that overlap any of the four $Nd^{3+}$ transitions from the $^4F_{3/2}$ state to the lower lying $^4I$ manifold (i.e. absorption in the 800 to 2000 nm range) are particularly troublesome. For this reason OH and certain transition metal ion impurities ($Cu^{2+}$, $Fe^{2+}$) are of most concern. The use of very high purity raw materials and melter refractories are required to remove the threat of transition metal impurities. Similarly, specific processing steps are added to eliminate OH from the glass melts [26, 30]; this dehydration step is one of the more difficult aspects of melting phosphate laser glasses because they tend to be hydroscopic.

Another important non-radiative loss mechanism is Nd-concentration quenching [56] (Fig 10). The mechanism entails energy transfer between two $Nd^{3+}$ ions, one in the $^4F_{3/2}$ excited state and the other in the $^4I_{9/2}$ ground state. The exchange converts both to the $^4I_{15/2}$ level from which they non-radiatively decay to the ground state. This non-radiative loss mechanism usually dominates at high Nd concentrations and is characterized by Q, the quenching factor. Q is defined as the concentration (ion/cm$^3$) that reduces the lifetime by one-half. Q is usually determined from emission lifetime measurements on a series of samples with different doping densities. The higher the Q value, the less sensitive (better) the laser glass is to Nd self-quenching. The degree of quenching generally increases as the square of the Nd doping level for

HEHP glasses and linearly for HAP glasses. Thus the units for Q as listed in Tables 3 and 4 reflect the specific functional dependence.

B. Non-linear refractive index

As discussed in section III, the performance of HEHP and Petawatt lasers can be limited by non-linear propagation effects, particularly at high irradiance. Locally, the refractive index increases in the presence of an intense laser beam as given by [3,5]:

$$n(I) = n_o + \gamma I \tag{9}$$

where $\gamma$ is the non-linear refractive index coefficient ($m^2/W$) and I is the laser irradiance ($W/m^2$). This can lead to self-focusing effects that can cause damage to the downstream laser glass or other optics. Self-focusing is generally divided into two types (Fig 11): 1) whole beam self-focusing that is a natural consequence of the Gaussian shape of many small-aperture laser beams and 2) localized self-focusing associated with spatial or temporal noise on the beam. For the case of whole-beam self-focusing, the higher intensities of the central regions of the beam induce a radial index-gradient (lensing effect) causing the whole beam to focus down on itself. At some point the irradiance exceeds the breakdown threshold of the material producing a damage spot in the optical material.

Localized self-focusing is similar in that high intensity noise spikes on a large-aperture beam collapse (focus) and generate associated damage on optics along the beam path. For example, damage commonly occurs on coated optics (e.g. mirrors and polarizers) and in the bulk glass of lenses and amplifier slabs along the beam propagation path.

The threat of non-linear noise growth is often expressed in term of the so-called "B-integral":

$$B = 2\pi/\lambda \int \gamma I(z)\, dz \tag{10}$$

where B (radians) is the cumulative non-linear phase retardation over the optical path length [5,58]. Intensity ripples (noise) that occur at certain spatial frequencies grow exponentially with B:

$$I = I_o \exp(B) \tag{11}$$

The greater the value of B, the greater the threat the beam will "break-up" into filaments as illustrated in Fig 11. In fact the use of the letter "B" to represent this term is an abbreviation for "break-up" [58]. Past experience has shown that B needs to be less than about 2 radians to avoid unacceptable noise ripple growth [59,60].

Direct measurement of $\gamma$ is difficult, so empirical correlations have been developed. The expression developed by Boling et al. [61] many years ago accurately predicts $\gamma$ from the refractive index ($n_d$) and the Abbe number ($\nu$) of the glass:

$$\gamma = K(n_d-1)(n_d^2+2)^2 / \{n_d \nu[1.52+(n_d^2+2)(n_d+1)\nu/6n_d]^{1/2}\} \tag{12}$$

where $K = 2.8 \times 10^{-10}$ $m^2/W$ and is an empirically determined constant.

Note that many researchers express Eq. 9 in terms of the non-linear refractive index, $n_2$ (in esu) rather than the more engineering friendly non-linear refractive index coefficient, $\gamma$ ($m^2/W$); for linear polarized light they are interrelated by $n_2 = \gamma (nc/40\pi)$ where n is the refractive index at the wavelength of interest.

C. Thermal-optical properties.

The laser glass must have high optical homogeneity to achieve the beam quality necessary to propagate and focus the laser output beam. Thermal variations in the laser glass can produce optical distortion by changing the optical path length. It is generally desirable to use a glass for which the temperature coefficient of the optical path length is zero; these are referred to as athermal glasses. The change in the optical path length, $\Delta O_L$, resulting from a temperature variation, $\Delta T$, over a length, L, is given by:

$$\Delta O_L = \delta L \Delta T \tag{13}$$

where $\delta$ is the temperature coefficient of the optical path length:

$$\delta = dn/dT + (n-1)\,\alpha_e \quad (14)$$

and (dn/dT) is the temperature change in refractive index relative to air and $\alpha_e$ is the coefficient of linear thermal expansion. An ideal athermal glass has $\delta = 0$ implying, from equation [14], $-dn/dT = (n-1)\,\alpha_e$. Therefore, a good athermal laser glass must have a negative dn/dT value about half the value of the coefficient of linear thermal expansion. Phosphate glasses are one of the few glass types that can be formulated to meet this condition.

D. Thermal-mechanical properties

Today's HEHP and PW laser systems tend to be essentially "single shot" devices with a few hours between shots; as a result the glass physical properties tend to be of less importance. In contrast, HAP lasers operate at substantial thermal loading associated with rep-rated operation. For this reason, good thermal-mechanical properties such as a high fracture toughness, high thermal conductivity and low thermal expansion are important. These properties are often collectively characterized in the well known "thermal shock resistance", $R_S$ ($W/m^{1/2}$) [62]:

$$R_S = k(1-\mu)K_{1C} / (E\,\alpha_e) \quad (15)$$

where E is Young's modulus (GPa), k the thermal conductivity (W/mK), $K_{1C}$ the fracture toughness (MPa $m^{1/2}$), $\mu$ Poisson's ratio and $\alpha_e$ the coefficient of linear thermal expansion ($K^{-1}$). The thermal shock resistance equates directly to the maximum thermal load that a surface-cooled glass slab can tolerate before catastrophic fracture [62,63]. Some versions of Eq. 15 include effects of surface flaws from finishing the glass; such flaws can seed fracture in externally cooled HAP glass plates.

E. Chemical Durability to "Weathering"

The resistance of glass to aqueous corrosion ("weathering") is important for all high-power laser applications. Glass durability is generally characterized by measuring the solubility of the glass in water under some well-defined condition.

For the case of HEHP and PW glasses, maximizing the glass composition to achieve high durability eases the problems encountered with finishing, cleaning, storing and handling the laser glass. The less durable glasses are more easily stained and fogged and can lead to optical damage or transmission losses or both. This in turn requires costly refinishing or the installation of expensive environmental controls within the laser system.

Glass durability requirements for HAP applications are even more demanding. HAP lasers are generally cooled with 100% de-ionized water or a mixture of de-ionized water and ethylene glycol and the amplifiers are expected to operate for years without maintenance or the need for slab replacement. Further complicating the durability issue is the threat of sub-critical crack growth from small surface flaws generated during optical finishing or from laser-induced damage. Such flaws can grow to large fractures in the presence of thermally-induced tensile stresses at the glass surface. As a consequence, HAP glasses are generally much more water durable than are HEHP compositions.

F. Laser damage resistance

The peak fluence in the laser glass of today's high power lasers can approach 5 to 20 J/cm$^2$ with a peak irradiance of up to 5.0 GW/cm$^2$. To avoid optical damage the laser glass surfaces must be precision polished and the bulk glass must be free of defects, specifically any microscopic inclusions that enter during processing. In most cases the inclusions originate from the refractory wall of the glass melter. HAP lasers face the added threat of crack initiation and growth at inclusion damage sites in the presence of thermally-induced tensile stress. In such cases the glass slab can catastrophically fracture [62].

The most common inclusions are ceramic or metallic particles from the liners used in the melting system. Platinum-lined melting vessels are usually required to prepare glasses with the high optical homogeneity needed for laser applications. However, the liners can generate trace concentrations of microscopic Pt metal particles in the glass. Although very small to begin with, inclusion damage can grow with successive laser shots to several millimeters or even centimeters in size eventually making the laser glass unusable. Also, large damage spots (> 0.3mm) in the laser glass can seed damage in other

optics in the laser chain. The presence of high levels of Pt inclusions typically found, for example, in silicates, borosilicates, and fluorophosphates, make these glasses unsuitable for high-energy laser applications. In contrast, inclusion-free laser glasses can be made using phosphate-based glass compositions melted under highly oxidizing conditions [26-28].

Today's laser glass melting systems are designed to both minimize inclusion generation and dissolve any residual inclusions in the glass. The effects of glass composition on platinum solubility have been reported to follow the trend: phosphate > silica-phosphate >> fluorophosphate > silicate [64]. These results are based on solubility measurements using LHG-5 and LHG-8 (phosphates), HAP-3 (silica-phosphate), LHG-10 (fluorophosphate) and LSG-91H (silicate). In a similar study, Hayden et al. [65] have examined the effects of the $Al_2O_3$ concentration in phosphate glasses on Pt solubility. They chose three commercial phosphate laser glasses (LG-770, LG-760 and APG-1), each having a different $Al_2O_3$ content. The effect of alumina was studied because it is a common modifier added to improve thermal-mechanical properties and is often added to HAP phosphate glasses. These researchers report that at higher $Al_2O_3$ concentrations the Pt solubility is reduced. The effect of $Al_2O_3$ on Pt solubility tends to parallel those reported by Izumitani for $SiO_2$ in Hoya HAP-3 glass [64]. This observation agrees with production melting experience in that HAP glasses are generally more difficult than HEHP glasses to manufacture Pt free.

Inspection methods have been developed and put into production to scan each piece of laser glass with a high fluence laser beam to detect the presence of inclusions [66].

If Pt inclusions are eliminated, the next limiting factor is the damage resistance of the polished glass surface [67]. Consequently optical material researchers have focused attention on further improving the quality of polished glass surfaces to increase the laser-damage-resistance. Work to date suggests that the onset of laser-induced surface damage is associated with residual subsurface defects and nano-scale contamination left from the polishing process [67-69]. The use of improved polishing methods in combination with post-polishing treatment of the surface to reduce or remove contamination and defects has shown promise for improving surface laser damage resistance for not only phosphate-based glasses

but also fused silica [70-71]. Fused silica is widely used for passive optic elements (such as lenses window and beam splitters) for high power lasers.

## V. Laser glass compositions

Development of improved laser glass compositions has been an active research field for more than 40 years. Composition studies have spanned a wide range of glass forming systems (silicates, phosphates, silicophosphates, fluorophosphates, and fluorides) and, in many cases, within each system the effects of variations in network modifiers have been studied (see, for example, [8] and sources cited therein).

The early laser glass composition work soon lead to phosphates as the glass of choice and today they are used in all high power glass laser systems around the world. Hundreds of different phosphate glass compositions have been melted in an effort to simultaneously optimize the laser properties while maintaining acceptable optical, thermal-mechanical and physical-chemical properties. Figure 12 is a ternary composition diagram for the $P_2O_5$-($Al_2O_3$, $RE_2O_3$)-(MO, $M_2O$) system showing the compositional region for high power laser glasses most widely used today. The HEHP glasses lie near the meta-phosphate join (O/P = 3) and have the approximate molar composition $60P_2O_5 – 10Al_2O_3$ - $30M_2O$/MO. Nd is added to this base composition at concentrations of about 0.2 mol% (~$5 \times 10^{19}$ ions/$cm^3$) for laser rods and up to 1-2 mol% (~2.5 to $5 \times 10^{20}$ ions/$cm^3$) for disks and plates.

The key properties of the most widely used commercial laser glasses are summarized in Table 3 and 4. The reported compositions for a few of the glasses are listed in Table 6; compositions for others remain proprietary. The range in component values account for small compositional variability due to doping and melting methods and to protect certain proprietary information. The reasons these specific modifiers and compositions make good laser glasses have recently been reviewed [8].

Like their HEHP counter-parts, HAP glasses have near meta-phosphate compositions, however the concentration of $Al_2O_3$ and/or $SiO_2$ is generally higher. These constituents give superior thermal-

mechanical properties to satisfy the heat loading experienced during HAP operations. Much of the compositional work on HAP glasses has focused on maximizing the glass thermal shock resistance (Eq. 15). The Nd-doping levels tend to be lower in HAP glasses, generally less than ~$2.5 \times 10^{20}$ ions/$cm^3$.

The general development approach for HAP glasses has been the following:

1) Improve the intrinsic thermal-physical properties by appropriate compositional changes or

2) Modify the glass composition to allow post-processing to improve strength (e.g. ion exchange) or

3) Do both.

Researchers at Schott have taken the compositional route and developed two high average power laser glasses: APG-1 developed in the 1980's [72], and a later version, APG- 2, jointly developed with LLNL [49]. APG-2 has a thermal shock resistance about 2.3 times greater than APG-1 (Table 4).

In another compositional study, workers at Hoya Corporation developed the silica-phosphate glass HAP-3[73,74] having the base composition $60P_2O_5$, $15SiO_2$, $10Al_2O_3$, $13Li_2O$, $2Nd_2O_3$ [52]. An improved version, HAP-4, was designed to be further strengthened by ion-exchange of the $Li^+$ for larger cations ($K^+$, $Na^+$) [75]. This exchange process generates a compressive residual stress at the surface. The compressive residual stress offsets the thermally-induced tensile stress that develops during operation, allowing the glass to tolerate greater thermal gradients.

HAP composition research at Kigre, Inc. led to a suite of ion-exchange strengthen $Er^{3+}$, $Yb^{3+}$ and $Nd^{3+}$ doped phosphate glasses. One such glass, Q-89, is a $BaO$-$Al_2O_3$-$P_2O_5$ meta-phosphate glass containing $Li_2O$ for ion-exchange strengthening [76,77].

Perhaps the most exciting new area of HAP glass development is the work by Fujimoto et. al. who report an Nd-doped high-silica glass made by a zeolite route [78-80]. The glass has small amounts of $Al_2O_3$ to enhance $Nd^{3+}$ incorporation in the structure. The $Al^{3+}$concentration is low enough that the glass retains the excellent thermal mechanical properties associated with the high-silica base. The properties of this developmental glass (Nd-SG) are included in the Table 4 summary of HAP glasses to illustrate the

much improved thermal shock resistance. Note that certain physical properties of the Nd-SG glass have been estimated by us from values for fused silica.

The zeolite route offers one possible method to avoid OH contamination that has plagued earlier attempts to fabricate Nd-doped silica glasses via a sol-gel route [81]. Recall from the early discussion (section IV.A) that residual hydroxyl contamination greatly accelerates the rate of non-radiative energy loss from the upper laser level ($^4F_{3/2}$) to OH vibrational modes [57]. Section VII discusses the role potential Nd:silica-type glasses could play in future high-energy laser development.

## VI. Laser Glass Manufacturing

To a large extent the development of high-energy and high-peak-power laser systems has been made possible by corresponding developments in advanced manufacturing technology. In the case of laser glass, there have been two key manufacturing developments that enabled the current class of HEHP lasers: continuous melting and high-speed optical finishing. These processes are the result of nearly ten years of manufacturing development done separately by Schott and Hoya, for glass melting and Zygo Corporation for glass finishing. This work was done in partnership with LLNL and funded by the US Department of Energy.

### A. Continuous melting

Prior to 2000, laser glass was melted in a two-step discontinuous process effectively producing one melt (i.e. glass slab) at a time and at a rate of only a few melts per week [82]. This technology, apart from being costly, was 20-times too slow to meet the demand for mega-joule scale HEHP laser systems. In addition, the quality of the product achieved with the discontinuous method can vary unpredictably from one melt to the next simply because of small run-to-run variations in processing conditions.

To meet the HEHP laser glass needs, Schott North America (Duryea, PA) and Hoya Corporation, USA (Fremont, CA) each developed continuous glass melting processes [26]. These two processes, which employ somewhat different proprietary melting technologies, are capable of producing between 70 to 300

glass blanks per week with better optical quality and at a significantly lower cost than possible with the prior pot-melting methods.

Although details of the Hoya and Schott melting systems differ, both carry out the same sequential set of processes. In brief, the continuous laser glass melting process converts high-purity, powdered raw materials into one continuously moving strip of high optical-quality laser glass (Fig. 13). The melting process requires several different operations carried out in separate, but interconnected vessels. The first process step is to mix and dry raw materials with minimal contamination. The laser glass specifications require that the raw materials contain only trace amounts ($\leq$10 ppm) of most common transition metal ions and less than 0.1 wt% of either physically or chemically absorbed water. The raw material is fed into the system where it dissolves into a pool of molten glass and is mixed by the convection currents inside the melter. The melter consists of custom designed high-purity refractory material and employs proprietary electrical heating systems.

All units beyond the melter are lined with platinum metal (99.9%), as are the interconnecting pipes. As mentioned in a previous section, platinum is required to achieve the part-per-million optical homogeneity necessary for laser applications, however platinum can contaminate the glass with microscopic metallic inclusions that can initiate laser damage sites (small fractures). To overcome this, a unique conditioner unit was developed that bubbles oxidizing gasses (oxygen and chlorine) through the melt with the dual purpose of dissolving platinum inclusions and minimizing residual hydroxyl contamination in the glass. The reduction in OH content dramatically improves the quantum efficiency. The conditioner unit is perhaps the most complex unit in the melting system.

The glass from the conditioner flows to a refiner section where bubbles are removed using proprietary additives in combination with quiescent conditions and high temperatures. From here the glass enters the homogenizer and is thoroughly mixed to achieve part-per-million levels of compositional uniformity resulting in an optical homogeneity of $\Delta n \lesssim 1\times10^{-6}$. The glass then flows through a platinum tube to a mold where it is formed into a continuously moving strip 5 to 8-cm thick and about 0.5-m wide.

The forming process is designed to produce straie free glass; straie are regions of high refractive index gradient caused by localized chemical or thermal inhomogeneity (or both). The strip slowly passes through a custom-designed annealing oven roughly 30 to 35-m long where the glass is gradually cooled from more than 600°C to room temperature. Glass "blanks", approximately 1 m × 0.5 m in size, are cut from the end of the strip as it exits the production system (Fig. 13). Each blank is fine annealed, inspected and fabricated into a pre-finished plate that is ready for final grinding and polishing (i.e. "finishing").

HAP glasses (APG-1and 2, HAP-3 and 4, Q89, etc.) are all manufactured using the 2-step discontinuous melting process. This is simply because the demand for these glasses is too small to warrant the expense of using continuous melting technology.

B. High-speed Optical Finishing

The goal of the finishing process is to produce a precision optic that can perform its design function (in this case, amplification) without impacting the overall laser beam quality. The beam quality can be adversely affected in three ways by the polished glass surface: (1) aberration of the transmitted wavefront, (2) scattering loss, and (3) laser damage. First, to reduce wavefront aberration the polishing process is used to correct for any large scale-length ($\gtrsim$2 cm) refractive index variations in the bulk glass [83]. This requires accurate removal of material from specific locations on the glass surface with a removal-depth accuracy of 10-100 nm. Second, to avoid scattering losses, the residual root-mean-square (rms) "roughness" of the polished surface typically must be less than 0.4 nm (4Å) [83]. Scattering from the glass surface can degrade the laser performance by: (a) reducing the output energy of the beam, (b) increasing the noise intensity that, in turn, increases the risk of laser damage due to intensity spikes ("hot spots"), and (c) irradiating surrounding mechanical hardware with scattered light and thus producing vapor or particulate blow-off. The blow-off can contaminate the optic surfaces leading to laser damage and a significant reduction in the useable life of the optic.

To achieve precision polished glass surfaces, the optic is finished in a series of steps using successively finer abrasives (Fig. 14). During the removal process, the interaction of the abrasive with the glass introduces subsurface defects (fractures) that extend below the glass surface. The goal of the subsequent material removal step is to not only reduce the surface roughness of the part, but also to remove sufficient material to get below the affected zone left from the prior step. In general this requires material removal to a depth 3-9 times the mean diameter of the abrasive used on the prior step. At the completion of final polishing, the goal is to remove all finishing-induced sub-surface defects and any residual nano-scale polishing contamination thereby achieving the greatest laser damage resistance and lowest scattering loss.

C. Application of Edge Cladding

Edge claddings are used to suppress parasitic oscillations of amplified spontaneous emission (ASE) during pumping of large pieces of laser glass [58]. Edge cladding consists of a refractive-index-matched glass that is doped (usually with $Cu^{+2}$) to absorb at the peak Nd-fluorescent wavelength. The cladding is bonded to the edges of the laser glass disks or slabs and absorbs the ASE, thereby preventing parasitic oscillations from developing. Adhesively-bonded edge claddings have been developed and are now widely used in the US, Europe and Japan [38, 84]. Two-part optical epoxies and polyurethanes are currently the most widely used adhesives. In general, epoxies are used for HEHP applications [84] whereas poly-urethanes are more commonly used for HAP lasers [38]. Poly-urethanes have good moisture resistance and are the best choice for the HAP water-cooled slabs. In contrast, the refractive index of optical epoxies can be very precisely modified to match the glass refractive index [84] and are a better choice for HEHP laser slabs with multi-kilojoules of stored energy.

D. Commercial suppliers

The laser glass market generally goes through “boom and bust” cycles that track the R&D and construction phases of the large HEHP laser projects across the world. Such cycles make it difficult for

private companies to maintain a commercial presence in the face of other pressing technical needs. For more than 30 years there have been three companies that have consistently supplied laser glasses for use in high-power lasers outside of China and Russia: Schott, Hoya and Kigre. Until 2007 Schott and Hoya had been the largest suppliers for the meter-scale glass pieces needed by the HEHP community. Hoya exited the laser glass business in 2007 leaving Schott as the only established commercial source for large sizes and quantities of laser glass. Similarly, Zygo Corporation is currently the only optical finishing company that can cut, clad, grind and polish meter-scale laser glass parts.

## VII. Glasses to meet future HEHP, HAP and PW laser needs

Future HAP and HEHP glass lasers will need to operate at higher repetition rates with the same or greater output energies. Consequently, improving the laser glass thermal shock resistance with minimum impact to other laser, optical and physical properties will become the main objective of future glass development. To help focus the discussion, Table 7 compares key thermal mechanical properties and the thermal shock resistance of today's commercial laser glasses with other common optical/laser materials.

The challenge for HAP lasers is more modest and may be met with modifications to the current suite of glasses. The HEHP requirement is more daunting and, as in the past, will necessitate government investment and support; it is clear that HAP and PW lasers will also benefit from that investment.

### A. HEHP Lasers for Fusion Energy Production

Proposed HEHP lasers for use in Inertial Fusion Energy (IFE) [85] and Fusion-Fission Hybrids (LIFE) [86, 87] call for drivers comprised of diode pumped mega-joule scale systems operating at ~10 Hz (10MW). Of course, current designs are still conceptual and clearly will evolve as new pump sources, optical materials and laser architectures are developed. Also, a future demonstration of PW driven fast-ignition [44] would greatly change the driver requirements.

Recall from section III that current HEHP laser systems operate every few hours (~$10^{-4}$ Hz). Therefore, achieving the ~$10^5$ increase in repetition rate needed for IFE power production will be a major

optical materials challenge. In particular, thermal shock resistance will be a key driver in the choice of a gain medium for the main amplifiers of fusion energy lasers.

Nd-glass is a current leading candidate for the gain media for IFE/LIFE lasers and a successful laser glass will require both HAP and HEHP properties. The best presently available commercial glasses are Schott's APG series (Table 4). However, surface imperfections and/or laser-induced damage in the glass could seed thermal fracture under the power loads at ~10Hz operation. Therefore, an inclusion-free gain medium with much higher Rs (10×) and acceptable laser properties would be a great benefit.

Apart from dramatically improved thermal mechanical properties, the gain medium must be manufactured in large volumes, free of damaging inclusions and with excellent optical quality. Mega-joule lasers require ~$10^5$ liters of gain medium (~300 tonnes) and production outputs of tonnes/day to be practical. Arguably, this requirement eliminates single-crystal gain media as an alternative to glass. Currently, the fastest growth rate achieved for large optical single-crystals is solution-growth of potassium di-hydrogen phosphate (KDP [88]). Plates of KDP (~40×40×1$cm^3$) cut from large single crystals are used for non-linear optical applications in today's HEHP laser systems. These crystals require two months to grow to the required ~500 lb size with an average growth rate of ~4kg/d. Although this rate represents a dramatic improvement in single crystal growth, it is ~1000 times lower than today's continuous optical glass melting rates. Moreover, KDP represents a best case; current high temperature crystal growth rates (as would be used for laser crystals) are much lower than the rate for KDP (perhaps 10-100× in the most optimistic cases). Therefore growth rate improvements of at least $10^3$ to $10^5$× would be needed for high-temperature single crystals to be practical.

In contrast, optical glass melting is a mature technology with demonstrated high production rates. Laser glass melting technology demonstrated tons per day for both LG-770 and LHG-8. This suggests that staying with Nd-glasses, but looking at alternatives with higher thermal shock resistance is a promising approach for early IFE laser development and deployment. This could be achieved by a two-pronged glass approach: one near term development effort aimed at improving current phosphate glasses

and the other a longer term effort to yield a greatly improved alternative. Both approaches are briefly discussed here.

1. Modified APG glasses to give higher $R_s$

The trend in APG glass development has been toward improving thermal mechanical properties while accepting some detrimental impact on laser properties, specifically lower cross-section and higher saturation fluence [49]. These glasses tend to be more difficult to manufacture than today's HEHP glasses because the APG compositions have greater melt viscosities and are more difficult to produce free of platinum particles. Nevertheless modest improvements in the thermal shock resistance (3-5×) appear possible without serious impact on laser properties while maintaining the production technology within reach.

One alternate development approach is to off-set the thermal burden on the laser glass with improved amplifier designs and associated cooling methods. The design of the next generation HEHP lasers is still largely conceptual and one can expect significant design improvements as these projects go forward. It is not unreasonable to expect future design improvements to significantly reduce the thermal shock requirements of the glass.

2. Nd-silica glasses

For decades it has been recognized that Nd-doped fused silica would make an excellent laser glass because of its high thermal shock resistance (Table 7) coupled with the ability to be manufactured inclusion-free in large sizes with excellent optical homogeneity. The difficulty has been achieving Nd-doping levels greater than $\sim 1 \times 10^{19}/cm^3$ without clustering; Nd clustering effectively quenches the radiative lifetime as discussed in section IV A and Figure 10. Arai et al. [89] showed that co-doping $SiO_2$ with $Al^{3+}$ via CVD inhibited Nd-clustering and thus opened up a new area of research on Nd-Al-$SiO_2$ glasses.

Subsequently, Thomas et al [81] used aNd-Al-$SiO_2$ sol-gel route to incorporate Nd followed by heating and sintering to densify the sample. Successful removal of residual OH was problematic and the quantum efficiency was low.

The work by Fujimoto et al. at Osaka University has produced, arguably, the most advanced of the Nd-Al-silica glasses to date [78-80]. These researchers use a zeolite route to incorporate Nd without clustering in a $SiO_2$ matrix with some $Al_2O_3$. They showed that the Nd remains in the un-clustered state after subsequent high temperature processing to densify the zeolite pre-form. Reported properties of this glass (glass code: Nd-SG) are listed in Table 4 and 7 for comparison with today's commercial HAP laser glasses. The thermal shock resistance is more than 50-times greater than current HEHP phosphate glasses. Although the authors originally developed the Nd-SG glass specifically for potential Fusion Energy laser applications [79] they also realize the potential for use in HAP lasers [78].

The Osaka Nd-Al-$SiO_2$ glass is a remarkable achievement and, in our opinion, represents an excellent starting point rather than end product for future IFE glass development. One reason it may not qualify as a final product is that compared with today's HEHP phosphate glasses the cross-section is lower ($1.4 \times 10^{-20}/cm^2$ vs. $\sim 3.5 \times 10^{-20}/cm^2$) and the associated saturation fluence higher (2.5×). The higher saturation fluence greatly increases the risk of optical damage in the main amplifier beam-path. However, it is likely that with a concerted development effort the composition could be altered to improve these important properties. There is a precedent and template for such an effort; for nearly 30 years the US Department of Energy funded glass development for Inertial Fusion Research resulting in today's phosphate laser glasses. In particular, systematic compositional studies were carried out in a partnership between the major optical glass companies with LLNL, the University of Rochester LLE and other laboratories. Measurements of laser, optical and physical properties were conducted on small samples using standard glass characterization methods. Many of these results are compiled in a set of glass catalogs published by Stokowski et al at LLNL [90]. Clearly such an approach to developing Nd-SG compositions would be warranted given the success by Fujimoto and co-workers. Parallel efforts in manufacturing development, again similar to what was done for phosphates, could also be undertaken. For example, an Nd-Al-$SiO_2$ sol-gel route, as explored earlier by Thomas et al. [81], may be possible with improved processing to remove residual OH.

B. Higher repetition-rate HAP lasers:

HAP lasers capable of KW outputs in high-quality ~20J single-pulses would offer significantly greater processing rates for materials processing, for example Laser Peening. The direction of future HAP glass research would closely follow any efforts made to address improved glasses for HEHP lasers. However, in contrast to HEHP, HAP laser systems may be able to compromise on some degradation in laser properties that would accompany significant improvement in thermal mechanical properties.

The manufacture of an improved phosphate HAP laser can, in principle, be carried out using today's glass melting technology. However, the manufacturing yields for inclusion-free glass, specifically platinum particle-free, will probably be reduced with the corresponding improvements of thermal mechanical properties [64].

Possible alternatives to phosphate glasses are Nd:Al-$SiO_2$ glasses similar to that being developed by Fujimoto et al as discussed above. These authors suggest a 100J, 10Hz laser (1 KW) is within reach [91] and list researchers at Shin-Etsu Quartz Products Co. as collaborators indicating a first step toward product commercialization. The viability of this alternative awaits publication of details on glass homogeneity and beam quality data.

C. Advanced Petawatt lasers

As discussed in section III C, PW lasers fall into two main categories: (i) table-top systems that fit into a large room and (ii) building-size systems that produce high-energies (>1kJ) as well as PW powers. The latter high-energy systems included the PW lasers associated with major HEHP facilities in the US, Japan, France, England and China as reviewed in section III A. In some aspects, the missions of the table-top and high energy systems differ although there is significant overlap.

The high-energy (~1kJ) lasers operate at longer pulse lengths making today's HEHP laser glasses acceptable for the time being. In fact, most high energy PW systems use amplifiers identical to those of the HEHP main laser system. Thus any new glasses for these systems will obviously benefit from corresponding future HEHP laser development as discuss above.

Table top PWs must operate at extremely short pulse lengths to achieve petawatt powers using only modest output energies. The push to exawatt powers ($10^{18}$W) with the associated sub 100-femotosecond pulse lengths is a challenge with today's HEHP glasses as discussed in section III C. New glasses with much broader band-widths are needed to handle shorter pulse lengths for the reasons discussed in section III. Nd-$SiO_2$ glasses are possible options, not because of the much greater thermal shock resistance, but due to the greater bandwidth (~50 nm [78]). Although a single glass would offer logistical advantages, the most promising approach, and one in use today [40], is to combine different glasses in series to achieve a larger effective emission bandwidth then offered by a single glass alone. The combination of current phosphate and silicate laser glasses with a very broad-band Nd-$SiO_2$ glass could significantly extend the effective operating bandwidth for future PW needs.

**Acknowledgements**

The authors gratefully acknowledge the helpful discussions with scientific and engineering staffs at Schott, LLNL and Metal Improvement Corporation. The valuable information provided by Dr. Yasushi Fujimoto on his work with Nd-silica is greatly appreciated.

**References**

1. E. Snitzer, "Optical maser action of $Nd^{3+}$ in a barium crown glass", Physical Review Letters, **7**, 444-446 (1961).

2. Interview of Dr. Elias Snitzer by Joan Bromberg on Aug. 6, 1984, Niels Bohr Library & Archives, American Institute of Physics, College Park, MD USA, www.aip.org/history/ohilist/LI.

3. W. Koechner, Solid-State Laser Engineering, 5th Ed., Springer-Verlag, New York, 1999.

4. B. E. A. Saleh and M. C. Teich, Fundamentals of Photonics, John Wiley and Sons, Inc., New York, 1991.

5. Antony Siegman, Lasers, University Science Books, Mill Valley, CA, 1986.

6. W. Koechner and M. Bass, Solid-State Lasers: A Graduate Text, Springer-Verlag, New York, 2003.

7. R.C. Powell, Physics of Solid-State Laser Materials, Springer-Verlag, New York, 1998, Chap. 9.

8. J. H. Campbell and T. I. Suratwala, "Nd-doped phosphate glasses for high energy/high power applications," J. Non-Cryst. Solids, **263&264**, 318-34 (2000).

9. J. D. Lindl, Inertial Confinement Fusion: The Quest for Ignition and Energy Gain Using Indirect Drive, Springer-Verlag, New York, 1998.

10. J. D. Lindl et al., "The physics basis for ignition using indirect-drive targets on the National Ignition Facility," Phys. Plasmas **11**, 339 (2004).

11. Hiroshi Azechi et al., "The FIREX Program on the Way to Inertial Fusion Energy," The Fifth International Conference on Inertial Fusion Sciences and Applications (IFSA2007) IOP Publishing, Journal of Physics: Conference Series **112** (2008) 012002 doi:10.1088/1742-6596/112/1/012002; 2008 J. Phys.: Conf. Ser. 112 012002 (http://iopscience.iop.org/1742-6596/112/1/012002)

12. Zheng Wanguo et al., "Status of the SG-III Solid-state Laser Facility," The Fifth International Conference on Inertial Fusion Sciences and Applications (IFSA2007) IOP Publishing, Journal of Physics: Conference Series **112** (2008) 032009 doi:10.1088/1742-6596/112/3/032009

13. X. T. He and W. Y. Zhang, "Inertial fusion research in China," Eur. Phys. J. **D** 44. 227–231 (2007) , DOI: 10.1140/epjd/e2007-00005-1

14. S. V. Grigorovich et al., "Prototype disc amplifier for ISKRA-6 facility," J. Phys. IV France **133**, 649-652 (2006) ; DOI: 10.1051/jp4:2006133129

15. J. Ebrardt and J. M Chaput, "LMJ on its way to fusion," The Sixth International Conference on Inertial Fusion Sciences and Applications, Journal of Physics: Conference Series **244** (2010) 032017 doi:10.1088/1742-6596/244/3/032017

16. T. R. Boehly et al., "Initial Performance results of the Omega Laser System," Optical Communications, **133**, 495-506 (1997)..

17. R. L. McCrory, D. D. Meyerhofer et al., "Progress in Direct-Drive Inertial Confinement Fusion Research," Phys. Plasmas **15 (5) (2008)**: 055503.

18. Bruno M. Van Wonterghem et al., "Performance of a prototype for a large-aperture multipass Nd:glass laser for inertial confinement fusion," Applied Optics, **36 (**21), 4932-495 (July, 20 1997).

19. Patrick K. Rambo et al., "Z-Beamlet: a multi-kilojoule, terawatt-class laser system," Applied Optics, **44 (12)**, 2421-2430 (April 20, 2005).

20. C. A. Haynam et al., "National Ignition Facility performance status," Applied Optics, **46**, 3276 (2007)

21. E. I. Moses, R. N. Boyd, B. A. Remington, C. J. Keane, and R. Al-Ayat, The National Ignition Facility: Ushering in a new age for high energy density science, Physics of Plasmas **16**, 041006 (2009)

22. Advanced Optics, SCHOTT North America, Inc., 400 York Avenue, Duryea, PA 18642 USA, www.us.schott.com/advanced_optics

23. HOYA Corporation USA**,** Optics Division**,** 3285 Scott Blvd.**,** Santa Clara, CA 95054 USA, www.hoyaoptics.com/contact/index.htm

24. KIGRE, Inc.*,* 100 Marshland Road, Hilton Head, SC 29926, USA. http://www.kigre.com/glass.html

25. Jing-ping Tang et al., "Properties of Phosphate Laser Glass by continuous melting", ACTA Photonica Sinica, **37**, 248-251 (2008).

26. J. H. Campbell et al., "Continuous melting of phosphate laser glasses", J. Non-Cryst. Solids, **263&264**, 342-357 (2000).

27. J. H. Campbell et al., "Elimination of platinum inclusions in phosphate laser glasses", Lawrence Livermore National Laboratory Report UCRL-JC-53932 (1989).

28. J. H Campbell et al., "Effects of process gas environment on platinum inclusion density and dissolution rate in phosphate laser glasses", Glastech. Ber. Glass Sci. Technol. **68 (2)**, 59-69 (1995).

29. J. H Campbell et al., "Effects of melting conditions on platinum inclusion content in phosphate laser glasses", Glastech. Ber. Glass Sci. Technol. **68 (1)**, 11-21 (1995).

30. C. B. Thorsness et al., "Dehydroxylation of Phosphate Laser Glass," SPIE **4102**, 175-194 (2000)...

31. T. Suratwala et al., "Technical advances in the continuous melting of phosphate laser glass," in Inertial Fusion Sciences and Applications, ed. K. Tanaka, D. Meyerhofer, J. Meyert-ter-Vehn, Elsevier (2002) 540-543.

32. E. I. Moses et al., "The National Ignition Facility: The World's Largest Optics and Laser System," SPIE **5001**, 1-15 (2003)..

33. G. H. Miller et al., "The National Ignition Facility," SPIE **5341**,, 84-101 (2004)..

34. K. Ding and L. Ye, Laser shock processing: performance and simulation, CRC press LLC, Boca Raton, FL 33487, USA (2006)

35. A. Kruusing, Handbook of liquids-assisted laser processing, Elsevier, Oxford, OX5 1GB, UK

36. Metal Improvement Company, Laser Peening Division, 7655 Longard Road, Livermore, CA 94551 http://www.metalimprovement.com/laserpeening.php

37. LSP Technologies, 6145 Scherers Place, Dublin, OH 43016-1284 http://lsptechnologies.com/

38. C. B. Dane et al., "Design and Operation of a 150 W Near Diffraction-Limited laser Amplifier with SBS Wavefront Correction," IEEE Journal of Quantum Electronics **31**, 148-163 (1995).

39. C. B. Dane et al., "High throughput laser peening of metals using a high-average-power Nd:glass laser system," International Forum on Advanced High Power Lasers and Applications, Osaka, Japan, November 1-5, 1999; LLNL report UCRL-JC-134266, Nov 1999, pp 1-13.

40. M. D. Perry and G. Mourou, "Terawatt to petawatt sub-picosecond lasers," Science, **264**, 917-924 (1994).

41. M. D. Perry et al., "Petawatt laser pulses", Optics Lett. **24**, 160-162 (1999).

42. G. A. Mourou et al., "Ultrahigh-Intensity Lasers: Physics of the Extreme on a Tabletop," Physics Today, **51**, 22–28 (1998).

43. D. Umstadter, "Review of Physics and Applications of Relativistic Plasmas Driven by Ultra-Intense Lasers," Physics of Plasmas, **8**, 1774–1785 (2001).

44. M. Tabak et al., "Ignition and high gain with ultra-powerful lasers", Physics of Plasmas, **1**, 1626 (1994).

45. International Committee on Ultra-high Intensity Lasers, http://www.icuil.org.

46. D. Strickland and G. Mourou, "Compression of amplified chirped optical pulses", Optics Communications, **56**, 219-221 (1985).

47. H. T. Nguyen et al., "Gratings for high-energy petawatt lasers", SPIE Boulder Damage Symposium XXXVII, Boulder, Co, USA (Sept. 19-23, 2005), LLNL Report UCRL-CONF-217007 (Nov. 11, 2005).

48. G. R. Hays et al., "Broad-spectrum neodymium –doped laser glasses for high-energy chirped-pulse amplification", Applied Optics, **46**, 4813-4819 (2007).

49. S. A. Payne et al., "Laser properties of a new average-power Nd-doped phosphate glass," Appl. Phys. B (Lasers and Optics), **B61**, 257-266 (1995).

50. S. A. Payne et al., "Spectroscopic properties of $Nd^{3+}$ dopant ions in phosphate laser glass," Ceramic Transactions: Solid State Optical Materials, **28**, 253-260, American Ceramic Society Press., (1992).

51. J. S. Hayden et al., "Effect of composition on the thermal, mechanical, and optical properties of phosphate laser glasses," High-Power Solid State Lasers and Applications, SPIE Vol. **1277**, 121-139 (1990).

52. H. Toratani, "Properties of laser glasses," Ph.D. Thesis, Kyoto University, Japan, (1989), pp. 1-187.

53. B. R. Judd, "Optical absorption intensities of rare-earth ions," Phys. Rev., **127**, 750 (1962).

54. G. S. Ofelt, "Intensities of crystal spectra of rare-earth ions," J. Chem. Phys., **37**, 511 (1962).

55. W. Krupke, "Induced emission cross-sections in neodymium laser glasses", IEEE J. Quantum Electronics, **QE-10**, 450 (1974).

56. P. R. Ehrmann and J. H. Campbell, "Nonradiative energy losses and radiation trapping in neodymium-doped phosphate laser glasses", J. Am. Ceram. Soc. **85**, 1061-69 (2002).

57. P. R. Ehrmann et al., "Neodymium fluorescence quenching by hydroxyl groups in phosphate laser glasses", J. of Non-Cryst. Solids, **349**, 105-114 (2004).

58. D. C. Brown, High-peak-power Nd:glass laser systems, Springer-Verlag, Berlin Heidelberg, 1981, p. 45.

59. J. T. Hunt and D. R. Speck, "Present and future performance of the Nova laser system," Optical Engineering, **28**, 461-468 (1989).

60. J. T. Hunt et al., "Hot images from obscurations," Applied Optics, **32**, 5973-5982 (1993).

61. N. L. Boling et al., "Empirical relationships for predicting non-linear refractive-index changes in optical solids," IEEE J. Quantum Electron. **QE-14**, 601 (1978).

62. J. Marion, "Appropriate use of the strength parameter in solid state slab laser design," J. Applied Phys., **60**, 69 (1986).

63. J. E. Marion, "Strengthened solid-state laser materials," Appl. Phys. Lett., **47 (7)**, 694-696 (1985).

64. T. Izumitani et al., "Solubility of Pt in Nd Phosphate laser glass," Laser Induced Damage in Optical Materials: 1987, NIST Special Publication **756**, 29-34 (1988).

65. Y. T. Hayden et al., "Effect of phosphate glass composition on the rate of platinum dissolution," Ceramic Transactions: Solid State Optical Materials, **28**, 283-296, Amer. Ceram. Society Press, (1992).

66. C. L. Weinzapfel et al., "Large scale damage testing in a production environment," Laser Induced Damage in Optical Materials: 1987, NIST Special Publication **756**, National Institute of Standards and Technology, 112-122 (1987).

67. J. H. Campbell, "Damage resistant optical glasses for high-power lasers: A continuing glass science and technology challenge," First international workshop on Glass and the Photonics Revolution, May 28-29, 2002, Bad Soden, Germany, Glass Sci. Technol. **75 C1**, 91-108 (2002).

68. P. E. Miller et al., "Fracture-induced sub-bandgap absorption as a precursor to optical damage on fused silica surfaces," Optics Letters, **35**, 2702-2704 (2010).

69. T. A. Laurence et al., "Metallic-like photoluminescence and absorption in fused silica surface flaws," Applied Physics Letters, **94**, 151114 (2009).

70. T. I Suratwala et al., "HF-based etching process for improving laser damage resistance of fused silica optical surfaces," J. Am. Ceram. Soc., **93**, 1-13 (2010).

71. T. I. Suratwala et al., "Toward deterministic material removal and surface figure during silica pad polishing," Am. Ceram. Soc., **93**, 1326-1340 (2010).

72. J. S. Hayden, D. L. Sapak, and H. J. Hoffman, "Advances in glasses for high average power laser systems," Conf. on High Power Solid State Lasers, SPIE, **1021**, 36-41 (1989).

73. T. Izumitani et al., "Development of silicophosphate glass, HAP-3," Laser Induced Damage in Optical Materials: 1986, NIST Special Publication **752**, 13 (1988).

74. C. Hata et al., “Chemically-strengthened slab laser glass with optical surface quality,” Laser Induced Damage Opt. Mater.: 1986, NIST Special Publication,, **752**, 168-175 (1988).

75. H. C. Lee and H. E. Meissner, “Ion-exchange strengthening of high average power phosphate laser glass,” SPIE **1441**, 87-103 (1991).

76. S. Jiang et al., “Chemically strengthened $Er^{3+}$, $Nd^{3+}$ doped phosphate laser glasses,” SPIE **2379**, 17-25 (1995).

77. U. Griebner et al., “Laser performance of a new ytterbium doped phosphate laser glass,” OSA Proc. of Advanced Solid State Lasers, , pp. 1-4 (1996).

78. Y. Fujimoto et al., “Development of Nd-doped optical gain material based on silica glass with high thermal shock parameter for high-average-power laser,” Jap. J. of Appl. Phys., **44**, 1764-1770 (2005)

79. Y. Fujimoto and M. Nakatsuka, “A novel method for uniform dispersion of the rare earth ions in $SiO_2$ glass using zeolite X,” J. Non-Cryst. Sol., **215,** 182-191 (1997).

80. T. Sato et al., “Laser oscillation of Nd-doped silica glass with high thermal shock parameter”, Jap. J. Appl. Phys., **45**, 6936-6939 (2006).

81. I. M. Thomas et al., “Optical properties and laser demonstrations of Nd-doped sol-gel silica glasses,” J. Non-Cryst. Solids, **151** 183-194 (1992).

82. A. J. Marker, "Optical glass technology," Geometrical Optics, SPIE Proceedings **531**, 2-10 (1985).

83. J. H. Campbell et al., "NIF Optical Materials and Fabrication Technologies: An Overview," SPIE **5341,** 85-101 **(**2004).

84. J. H. Campbell et al., "Development of Composite polymer-glass edge claddings for NOVA laser disks," H. E. Bennett, A. H. Guenther, D. Milam, and B. E. Newnam, Eds., Damage in Laser Materials:1986, NIST (U.S.) Special Publication, **752** 19-41 (1987).

85. M. Yamanaka et al., "Laser-diode pumped 10J × 10Hz Nd:glass slab laser for inertial fusion energy," Inertial Fusion Sciences and Applications 99, Editors: Labaune, C., Hogan, W. J., Tanaka, K. A., Elsevier, Paris 644-649 (2000).

86. E. I. Moses et al., "A sustainable nuclear fuel cycle based on laser inertial fusion energy," Fusion Science and Technology, **56**, 547-565 (2009).

87. J. Caird et al., "Nd:glass laser design for laser ICF fission energy (LIFE)," Fusion Science and Technology, **56**, 607-617 (2009).

88. N. Zaitseva and L. Carmen, "Rapid growth of KDP-type crystals," Prog. Cryst. Growth Charact. Mater., **43**, 1-118 (2001).

89. K. Arai et al., "Aluminum or phosphorus co-doping effects on the fluorescence and structural properties of neodymium-doped silica glass," J. Appl. Phys. **59**, 3430 (1986).

90. S. E. Stokowski et al., “Nd-doped laser glass spectroscopic and physical properties,” Lawrence Livermore National Laboratory Report **M-095**, Rev. 2 Vol. 1 and 2 (1981).

91. T. Sato et al., “40J-class laser oscillation of Nd-silica glass with high thermal shock parameter,” Applied Physics Letters, **90**, 221108 (2007) doi:10.1063/1.2744487.

Table 1. The three main categories of high-power glass lasers in operation today and typical operating characteristics

| | **Typical laser output characteristics** | | | |
|---|---|---|---|---|
| **Category** | **Energy (J)** | **Pulse length (s)** | **Peak power (W)** | **Repetition rate (Hz)** |
| High-Energy/High Power (HEHP) | $10^{5} – 10^{6}$ | $10^{-9} – 10^{-8}$ | $10^{13} – 10^{15}$ | $10^{-4} – 10^{-5}$ |
| Petawatt (PW) | $10^{2} – 10^{3}$ | $10^{-14} – 10^{-13}$ | $> 10^{15}$ | $10^{-4} – 10^{-5}$ |
| High Average Power (HAP) | $10 – 10^{2}$ | $10^{-9} – 10^{-8}$ | $10^{10}$ - $10^{11}$ | 1 - 10 |

Table 2. Examples of multi-kilojoule HEHP glass laser systems in operation, under construction, or proposed.

| Laser Facility and Status | Location | Phosphate glass type | Laser output at 1.05 μm (kJ) | Laser output at 0.35 μm (kJ) |
|---|---|---|---|---|
| **I. Operational** | | | | |
| NIF | LLNL | LG-770/LHG-7 | 3000 | 1800 |
| Omega | Univ. of Rochester | LHG-8 | 54 | 30 |
| Omega-EP | Univ. of Rochester | LHG-8 | 2.7 | NA |
| Gekko-XII | Osaka, Japan | LHG-8 | 12 | 10[a] |
| Beamlet | LLNL/Sandia NL | LG-750 | 17 | 10 |
| LFEX (PW) | Osaka, Japan | LHG-8 | 1 | NA |
| Shenguang (SG)-IIU | China | N-31 | 30 | 18 |
| Vulcan | UK | LG-770/LHG-8 | 2.5 | 1[a] |
| LIL | France | LHG-8/LG-750/LG-770 | 40 | 20 |
| **II. Under Construction** | | | | |
| LMJ | France | LG-770/LHG-8 | 1200 | 900 |
| FireX | Osaka, Japan | LHG-8 | 50 | ? |
| Shenguang (SG)-III-TIL | China | N-31 | 30 | 15-20 |
| Shenguang (SG)-III | China | N-31 | 300 | 150-200 |
| **III. Proposed** | | | | |
| ISKRA-6 | Russia | KGSS-0180/35 grade | 600 | ? |
| Shenguang (SG)-IV | China | undetermined | 3000 | 1500-2000 |
| LIFE | LLNL | undetermined | 2000 | 1000 |
| HiPER | UK | undetermined | 270 | ? |

[(a)] at 532nm

Table 3: Properties of most commonly used commercial HEHP glasses

| Glass Manufacturer | | Hoya [23] | | | Schott [22] | | | Kigre [24] | |
|---|---|---|---|---|---|---|---|---|---|
| Glass Properties | Symbol | LHG-80 | LHG-8 | LHG-5 | LG-770 | LG-750 | LG-760 | Q88 | Q98 |
| **Optical** | | | | | | | | | |
| refractive index | | | | | | | | | |
| @ 587.6 nm | $n_d$ | 1.5429 | 1.5296 | 1.5410 | 1.5067 | 1.5257 | 1.519 | 1.5449 | 1.555 |
| @ 1053 nm | $n_l$ | 1.5329 | 1.5201 | 1.531 | 1.4991 | 1.5160 | 1.508 | 1.5363 | 1.546 |
| non-linear refractive index | | | | | | | | | |
| ($10^{-13}$ esu) | $n_2$ | 1.24 | 1.12 | 1.28 | 1.01 | 1.08 | 1.02 | 1.14 | 1.2 |
| ($10^{-20}$ $m^2$/W) | $\gamma$ | 3.36 | 3.08 | 3.52 | 2.78 | 2.98 | 2.82 | 3.11 | 3.3 |
| Abbe number | $\nu$ | 64.7 | 66.5 | 63.5 | 68.4 | 68.2 | 69.2 | 64.8 | 63.6 |
| Temp-coeff. refract. index ($10^{-6}$/K) | dn/dT | -3.8 | -5.3 | -0.4 | -4.7 | -5.1 | -6.8 | -0.5 | -4.5 |
| Temp-coeff. optical path ($10^{-6}$/K) | $\delta$ | 1.8 | 0.6 | 4.2 | 1.2 | 0.8 | -0.4 | 2.7 | 0 |
| **Laser**[a] | | | | | | | | | |
| emission cross-section($10^{-20}$$cm^2$) | $\sigma_{em}$ | 4.2 | 3.6 | 4.1 | 3.9 | 3.7 | 4.6 | 4.0 | 4.5 |
| saturation fluence (J/$cm^2$) | $F_{sat}$ | 4.5 | 5.2 | 4.6 | 4.8 | 5.1 | 4.1 | 4.7 | 4.2 |
| radiative lifetime (zero-Nd) (μs) | $\tau_o$ | 337 | 365 | 320 | 372 | 383 | 330 | 326 | 308 |
| Judd-Ofelt radiative lifetime (μs) | $\tau_r$ | 327 | 351 | 320 | 349 | 367 | 320 | 326 | — |
| emission band width (nm) | $\Delta\lambda_{eff}$ | 23.9 | 26.5 | 26.1 | 25.4 | 25.3 | 23.5 | 21.9 | 25.5 |
| conc. quenching factor ($cm^{-3}$)[a] | Q | 10.1 | 8.4 | 8.5 | 8.8 | 7.4 | 10 | 6.6 | |
| fluorescence peak (nm) | $\lambda_L$ | 1054 | 1053 | 1054 | 1053 | 1053 | 1054 | 1054 | 1053 |
| **Thermal** | | | | | | | | | |
| thermal conduct., (W/mK) (298K) | k | 0.63 | 0.58 | 0.77 | 0.57 | 0.49 | 0.57 | 0.84[c] | 0.82[c] |
| thermal diffusivity($10^{-7}$ $m^2$/s) | $D_T$ | 3.2 | 2.7 | — | 2.9 | 2.9 | 3.0 | — | — |
| specific heat, (J/gK) | $C_p$ | 0.63 | 0.75 | 0.71 | 0.77 | 0.72 | 0.75 | 0.81 | 0.80 |
| Coeff. thermal expan. ($10^{-7}$/K)[b] | $\alpha_e$ | 130 | 127 | 98 | 134 | 132 | 150 | 104[d] | 99[d] |
| Glass transition temp (°C) | $T_g$ | 402 | 485 | 455 | 460 | 450 | 350 | 367 | 416 |
| **Mechanical** | | | | | | | | | |
| density (g/$cm^3$) | ρ | 2.92 | 2.83 | 2.67 | 2.59 | 2.83 | 2.60 | 2.71 | 3.10 |
| Poisson's ratio | μ | 0.27 | 0.26 | 0.24 | 0.25 | 0.26 | 0.27 | 0.24 | 0.24 |
| Fracture toughness (MPa $m^{0.5}$) | $K_{1C}$ | 0.46 | 0.51 | 0.42 | 0.48 | 0.45 | 0.47 | — | — |
| Hardness (GPa) | H | 3.35 | 3.43 | 4.2 | 3.58 | 2.85 | 3.18 | — | — |
| Young's modulus (GPa) | E | 50.1 | 50.1 | 67.7 | 47.3 | 50. | 53.7 | 70.1 | 72.1 |
| Thermal shock resistance (W/$m^{1/2}$) | $R_s$ | 0.32 | 0.25 | 0.37 | 0.32 | 0.30 | 0.24 | - | - |

[a] Nd self-quenching increases quadratically as $[Nd/Q]^2$; see text

[b] 20-300°C unless otherwise stated

[c] Temperature not specified

[d] 20-40°C

Table 4. Properties of commercial HAP glasses and one developmental glass by Fujimoto et al. (Nd-SG) [78]

| Glass Manufacture | | Kigre [24] | Schott [22] | | Hoya [23] | | Devel. [78] |
|---|---|---|---|---|---|---|---|
| Glass Properties | Symbol | Q89-Nd | APG-1 | APG-2 | HAP-4 | HAP-3 | Nd-SG |
| **Optical** | | | | | | | |
| refractive index | | | | | | | |
| @ 587.6 nm | $n_d$ | 1.559 | 1.537 | 1.5127 | 1.5433 | 1.5298 | 1.4584 |
| @ 1053 nm | $n_l$ | | 1.526 | 1.5032 | 1.5331 | 1.5200 | 1.4496 |
| non-linear refractive index | | | | | | | |
| ($10^{-13}$ esu) | $n_2$ | | 1.13 | 1.06 | 1.21 | 1.09 | 0.87 |
| ($10^{-20}$ $m^2$/W) | $\gamma$ | | 3.1 | 2.85 | 3.32 | 3.0 | 2.39 |
| Abbe number | $\nu$ | 63.6 | 67.7 | 66.9 | 64.6 | 67.7 | 67.9 |
| Temp-coeff. refract. index ($10^{-6}$/K) | dn/dT | — | 1.2 | 3.4 | 1.8 | 1.9 | — |
| Temp-coeff. optical path ($10^{-6}$/K) | $\delta$ | — | 5.2 | 7.6 | 5.7 | 5.7 | — |
| **Laser** | | | | | | | |
| emission cross-section ($10^{-20}$ $cm^2$) | $\sigma_{em}$ | 3.8 | 3.4 | 2.4 | 3.6 | 3.2 | 1.4 |
| Saturation Fluence (J/$cm^2$) | $F_{sat}$ | 5.0 | 5.6 | 7.9 | 5.3 | 5.9 | 13.4 |
| radiative lifetime (zero-Nd) (μs) | $\tau_o$ | 350 | 385 | 464 | 350 | 380 | 376(?) |
| Judd-Ofelt radiative lifetime (μs) | $\tau_r$ | — | 361 | 456 | — | 372 | 512[d] |
| emission band width (nm) | $\Delta\lambda_{eff}$ | 21.2 | 27.8 | 31.5 | 27.0 | 27.9 | 51.7 |
| conc. quenching factor ($cm^{-3}$)[a] | Q | — | 16.7 | 10.6 | — | — | — |
| fluorescence peak (nm) | $\lambda_L$ | 1054 | 1053.9 | 1054.6 | 1054 | 1052.5 | 1062 |
| **Thermal** | | | | | | | |
| thermal conduct., (W/mK) (90°C) | k | 0.82 | 0.83 | 0.84 | 1.02 | 0.8 | 1.38 |
| thermal diffusivity($10^{-7}$ $m^2$/s) (90°C) | $D_t$ | — | 3.5 | 4.1 | 5.2 | — | 7.5 |
| specific heat, (J/gK) | $C_p$ | — | 0.84 | 0.77 | 0.71 | — | 0.74 |
| Coeff. thermal expan.($10^{-7}$/K)[b] | $\alpha_e$ | 88 | 99.6 | 64 | 72 | 75 | ~1 |
| Glass transition temp (°C) | $T_g$ | 440 | 450 | 549 | 486 | 541 | — |
| **Mechanical** | | | | | | | |
| density (g/$cm^3$) | $\rho$ | 3.14 | 2.64 | 2.56 | 2.70 | 2.66 | 2.20 |
| Poisson's ratio | $\mu$ | — | 0.24 | 0.24 | 0.24 | 0.23 | 0.16 |
| Fracture toughness (MPa $m^{0.5}$) | $K_{1C}$ | — | 0.60 | 0.64 | 0.83 | 0.48 | 0.80 |
| Hardness (GPa) | H | — | 3.09 | — | 4.7 | — | — |
| Young's modulus (GPa) | E | — | 71 | 64 | 70 | 75.2 | 72.7 |
| Thermal shock resistance (W/$m^{1/2}$) | $R_s$ | — | 0.70 | 1.02 | 1.28 | 0.52 | ~20 est. |

[a]Nd self-quenching increases linearly as [Nd/Q]; see text

[b] 20-300°C

[c] Thermal mechanical properties estimated from values for fused silica

[d] Computed by authors using J.O. treatment of reported spectral data in [78]

Table 5. Properties of commercial laser glasses in use on some PW systems and proposed glasses for future use.

| Glass Code | Cross-section $\sigma$ [$10^{-20}$ $cm^2$] | Bandwidth, $\Delta\lambda_{eff}$ [nm] | Radiative lifetime $\tau_{rad}$[μs] | Non-linear refractive index $n_2$ [$10^{-13}$ esu] | Saturation fluence $F_{sat}$[$J/cm^2$] | Glass type |
|---|---|---|---|---|---|---|
| **I. Commercial** | | | | | | |
| APG-1 [a] | 3.4 | 27.8 | 361 | 1.03 | 5.6 | phosphate |
| APG-2 [a] | 2.4 | 31.5 | 456 | 1.06 | 7.9 | phosphate |
| LG-750 [a] | 3.7 | 25.3 | 367 | 1.08 | 5.1 | phosphate |
| LG-770 [a] | 3.9 | 25.4 | 349 | 1.01 | 4.8 | phosphate |
| LG-680 [a] | 2.5 | 35.9 | 361 | 1.60 | 7.5 | silicate |
| Q246 [b] | 2.4 | 28.5 | 406 | 1.49 | 7.0 | silicate |
| **II. Devel.** | | | | | | |
| Nd-SG [c] | 1.4 | 51.7 | 512 | 0.87 | 13.4 | silica |
| L65 [d] | 1.8 | 41.2 | 349 | 2.92 | 10 | aluminate |
| K824 [d] | 2.4 | 38.2 | 274 | 3.44 | 7.0 | Ta-silicate |
| | | | | | | |

[a] Schott [22]

[b] Kigre [24]

[c] Fujimoto [78]

[d] LLNL glass catalog [90]

Table 6. Representative compositions of commercial HEHP and HAP Nd-doped phosphate laser glasses and one developmental glass, Fujimoto et al. (Nd-SG) [78]

| **Component oxide equivalent (mol%)** | **LHG-8 [8]** | **LG-770 [8]** | **LG-750 [8]** | **HAP-3 [52]** | **Nd-SG [78]** |
|---|---|---|---|---|---|
| $P_2O_5$ | 55-60 | 58-62 | 55-60 | 60 | - |
| $Al_2O_3$ | 8-12 | 6-10 | 8-12 | 10 | 1.64 |
| $SiO_2$ | - | - | - | 15 | 98.1 |
| $K_2O$ | 13-17 | 20-25 | 13-17 | - | - |
| $Li_2O$ | - | - | - | 13 | - |
| BaO | 10-15 | - | 10-15 | - | - |
| MgO | - | 5-10 | - | - | - |
| $Nd_2O_3$[a] | 0-2 | 0-2 | 0-2 | 0-2 | 0.23 |
| Other | <2 | <2 | <2 | <2 | 0 |
| O/P ($\pm$0.1) | 3 | 3 | 3 | 3.2 | NA |

[a.] Nd-doping levels vary depending on use.

Table 7: Thermal mechanical properties and the computed thermal shock resistance (Eq. 15) for common commercial phosphate laser glasses and other well known laser optical materials.

| Material | Fracture toughness $K_{1c}$ ($MPa*m^{1/2}$) | Thermal conductivity k (Wm/K) | Poisson's ratio $\mu$ | Young's modulus E GPa | thermal expan $\alpha$ $10^{-6}$ $K^{-1}$ | Thermal Shock Res. $R_s$ $W/m^{1/2}$ | Improvement vs. LG-770 |
|---|---|---|---|---|---|---|---|
| **I. HEHP Glasses** | | | | | | | |
| LHG-8 | 0.51 | 0.58 | 0.26 | 50 | 12.7 | 0.34 | NA |
| LG-750 | 0.45 | 0.49 | 0.26 | 50 | 13.2 | 0.25 | NA |
| LG-770 | 0.48 | 0.57 | 0.25 | 47.3 | 13.4 | 0.32 | 1.0 |
| **II. HAP Glasses** | | | | | | | |
| APG-1 | 0.6 | 0.83 | 0.24 | 71 | 7.6 | 0.70 | 2.2 |
| APG-2 | 0.64 | 0.86 | 0.24 | 64 | 6.4 | 1.02 | 3.2 |
| HAP-3 | 0.48 | 0.8 | 0.23 | 75.2 | 7.5 | 0.52 | 1.6 |
| HAP-4 | 0.83 | 1.02 | 0.24 | 70 | 7.2 | 1.28 | 3.9 |
| **III. Silica glasses** | | | | | | | |
| ED-2 | 1.1 | 1.35 | 0.24 | 91.9 | 8 | 1.54 | 4.7 |
| Fused Silica | 0.8 | 1.3 | 0.16 | 72.7 | 0.55 | 21.8 | 67.5 |
| **IV. Crystals** | | | | | | | |
| YAG | 2.2 | 13 | 0.28 | 282 | 8 | 9.13 | 28.2 |
| $Al_2O_3$ (sapphire) | 2 | 40 | 0.28 | 400 | 8.5 | 16.9 | 52.3 |

**Figure Captions**

Figure 1. Schematic representation of (a) laser oscillator and (b) oscillator plus amplifier

Figure 2. Schematic representation of a flashlamp-pumped amplifier containing rectangular slabs of laser-glass gain media.

Figure 3. (a) Engineering and (b) atomistic representations of flashlamp pumping, Nd excitation, relaxation and stimulated emission (amplification) in $Nd^{3+}$ doped laser glass.

Figure 4. Photograph of one of the two laser bays of the NIF; note the workers in the lower left corner for scale. Each bay accommodates half of the 192 individual laser beams that comprise the NIF laser system. The ~40×40 cm aperture laser beams are transported in large diameter pipes clearly visible in the photo. The main laser amplifiers are assembled in the laser bay at given positions along the beamlines.

Figure 5. (a)Precision laser glass plates are assembled in (b) cassettes for installation on the NIF. A total of 768 such cassettes are used in the NIF amplifiers.

Figure 6. Schematic representation of the laser shock peening process showing (a) the laser pulse incident on the work piece, and (b) the resulting high pressure ablation plasma and subsequent pressure (shock) that propagates through the material.

Figure 7. Highly schematic representation of a flashlamp pumped zig-zag amplifier commonly used on HAP laser systems

Figure 8. Schematic representation of a typical Petawatt CPA design showing the short pulse temporal expansion, amplification and compression.

Figure 9. (a) $Nd^{3+}$ absorption spectrum, (b) emission spectrum and (c) emission transient for a typical $Nd^{3+}$-phosphate glass. The emission transient is used to determine the emission lifetime, $\tau_{meas}$. Non-radiative energy losses reduce the lifetime and the quantum efficiency as discussed in the text and in Fig 10.

Figure 10. Schematic representation of major mechanisms for non-radiative energy loss from the $^4F_{3/2}$ state (i.e. upper laser level): (a) Nd-to-Nd energy transfer (self-quenching), (b) energy transfer to OH vibrational modes and (c) transition metal vibronic excitations.

Figure 11. Illustration of (a) whole beam and (b) localized self-focusing during propagation of a high intensity laser beam through an optical material of refractive index n(I).

Figure 12. Ternary composition diagram for the $P_2O_5$-$Al_2O_3$/$RE_2O_3$-MO/$M_2O$ system showing the approximate compositional region (as indicated by the spot) for most commercial HEHP and HAP laser glasses. These glasses have an O/P ratio of about 3/1 (i.e. "meta-phosphate") implying a backbone structure of rings and long chains of $PO_3$ groups. The units of the plot are in mole fraction.

Fig. 13. Schematic representation of the continuous melting process used to prepare HEHP laser glass blanks from which finished laser slabs are fabricated.

Fig. 14. Optical "finishing" uses a combination of grinding and polishing steps that successively remove material from the glass surface in incrementally smaller amounts. The goal is to remove sufficient material to eliminate all subsurface fractures (defects) produced by the previous step. The subsurface

damage is generally less than 1um deep and widely dispersed at completion of the final precision polishing step.

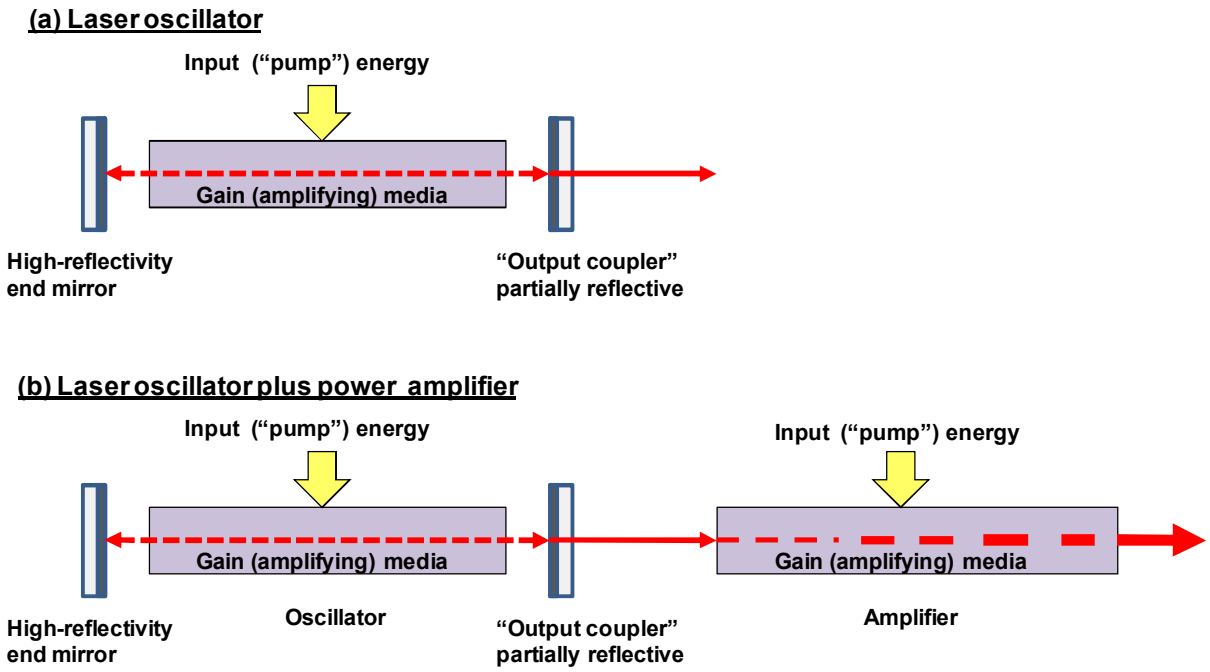


Figure 1. Schematic representation of (a) laser oscillator and (b) oscillator plus amplifier.

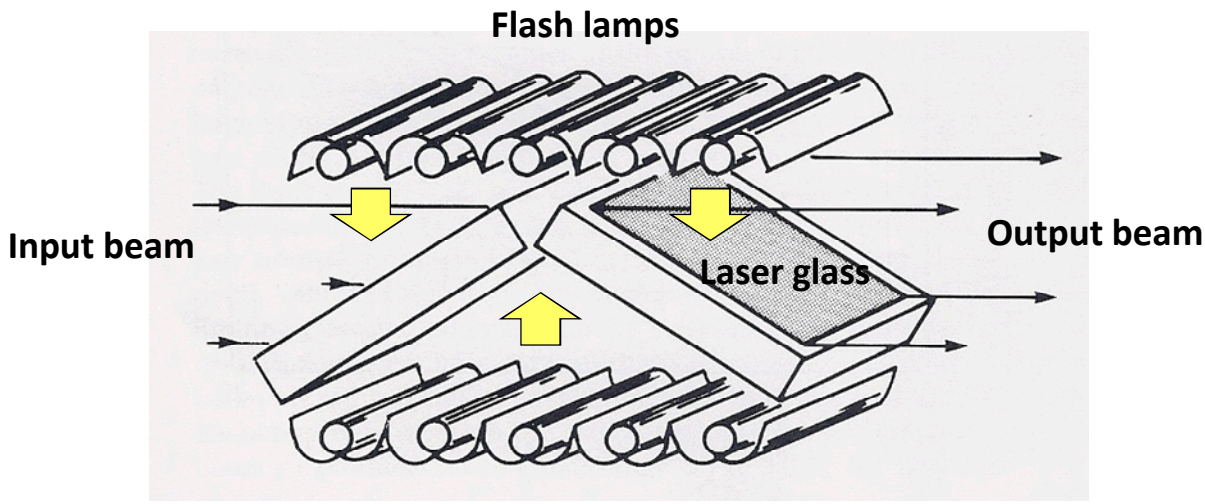


Figure 2. Schematic representation of a flashlamp-pumped amplifier containing rectangular slabs of laser-glass gain media

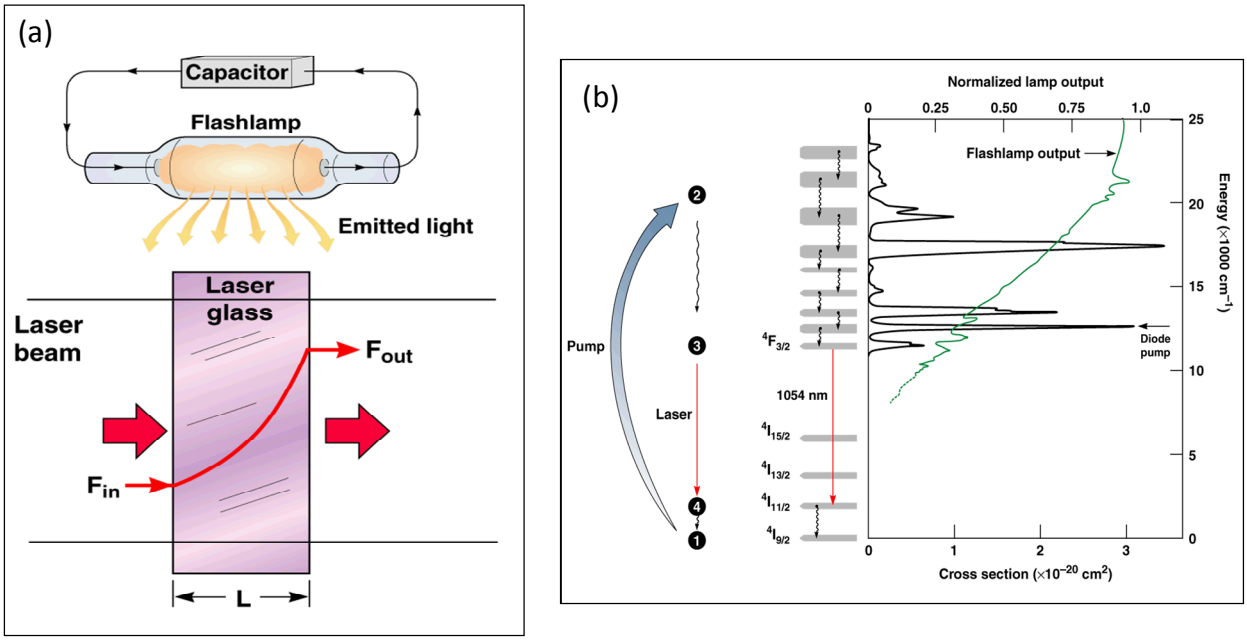


Figure 3. (a) Engineering and (b) corresponding representations of flashlamp pumping, Nd excitation, relaxation and stimulated emission (amplification) in $Nd^{3+}$ doped laser glass.

Figure 4. Photograph of one of the two laser bays of the NIF; note the workers in the lower left corner for scale. Each bay accommodates half of the 192 individual laser beams that comprise the NIF laser system. The ~40×40 cm aperture laser beams are transported in large diameter pipes clearly visible in the photo. The main laser amplifiers are assembled in the laser bay at given positions along the beamlines.

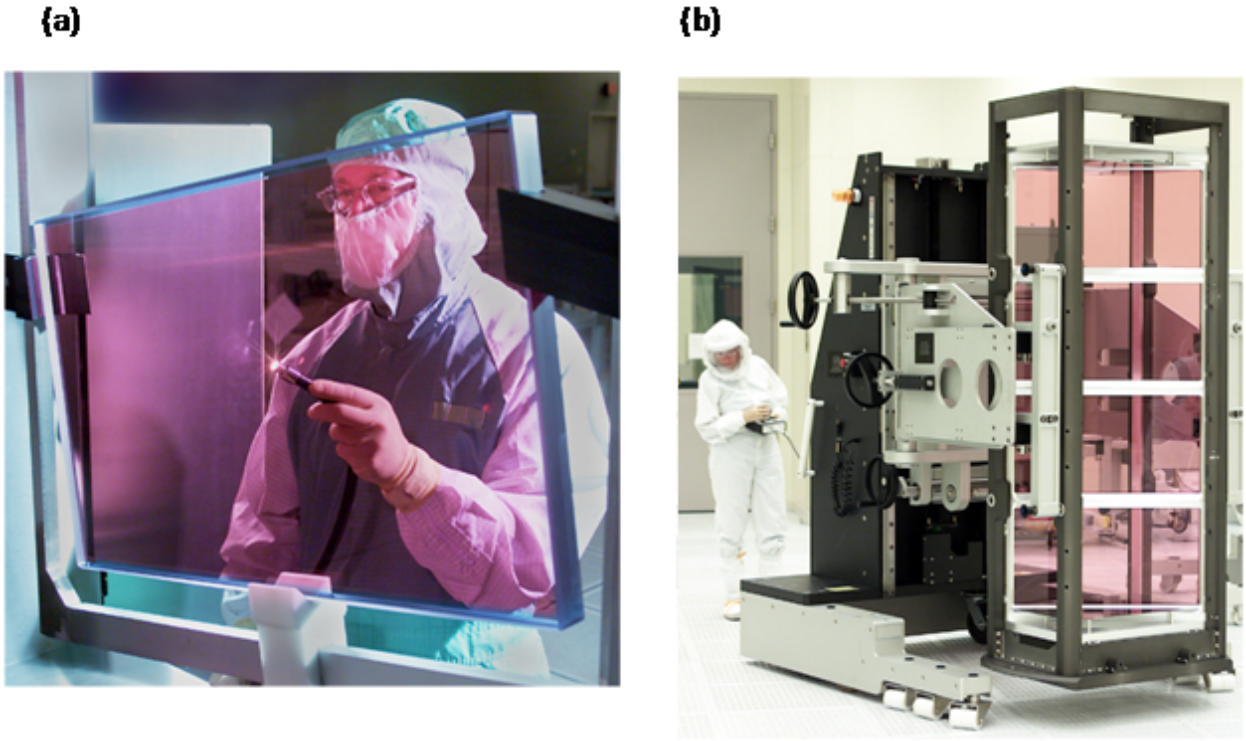


Figure 5. (a) Precision laser glass plates are assembled in (b) cassettes for installation on the NIF. A total of 768 such cassettes are used in the NIF amplifiers.

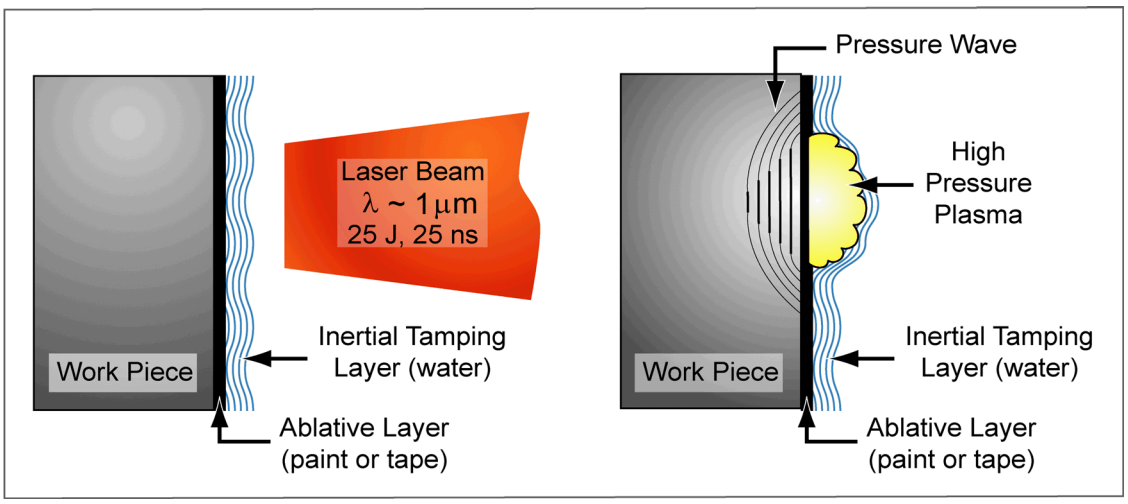


Figure 6. Schematic representation of the laser shock peening process showing (a) the laser pulse incident on the work piece and (b) the resulting high pressure ablation plasma and subsequent pressure (shock) that propagates through the material.

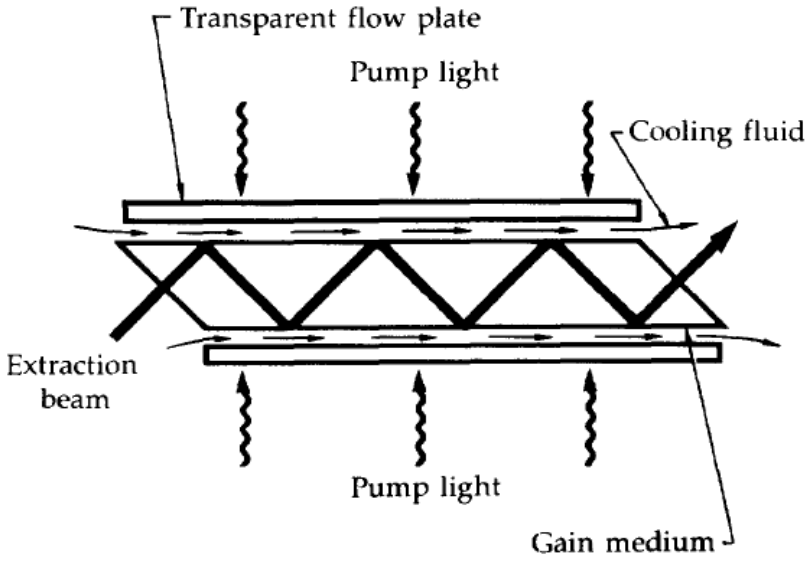


Figure 7. Highly schematic representation of a flashlamp pumped zig-zag amplifier commonly used on HAP laser systems.

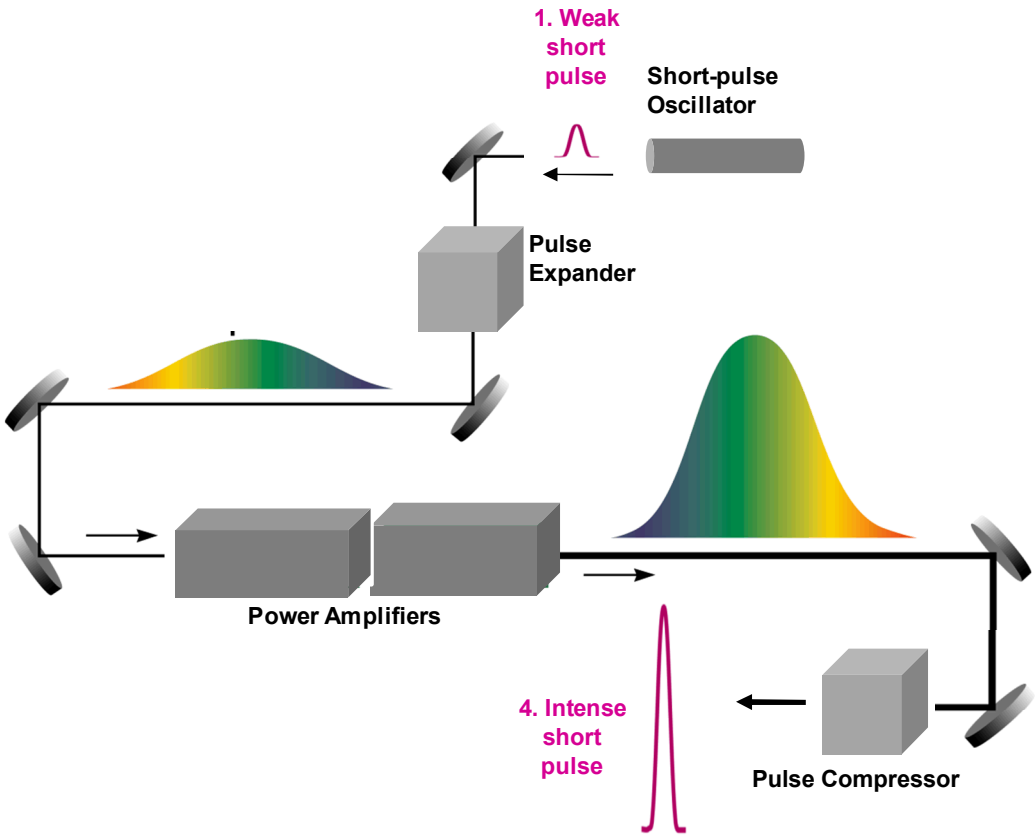


Figure 8. Schematic representation of a typical Petawatt CPA design showing the short pulse temporal expansion, amplification and compression.

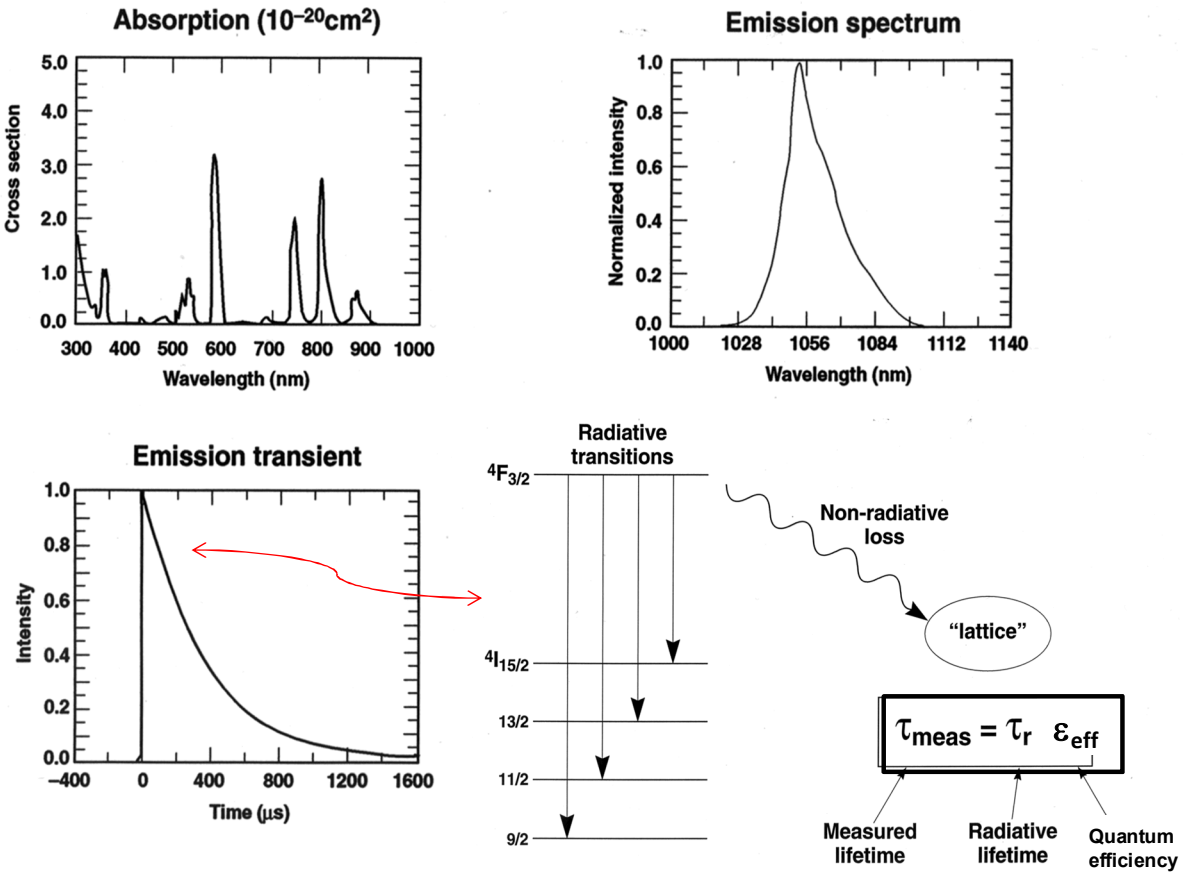


Figure 9. (a) $Nd^{3+}$ absorption spectrum, (b) emission spectrum and (c) emission transient for a typical $Nd^{3+}$-phosphate glass. The emission transient is used to determine the emission lifetime, $\tau_{meas}$. Non-radiative energy losses reduce the lifetime and the quantum efficiency as discussed in the text and in Fig 10.

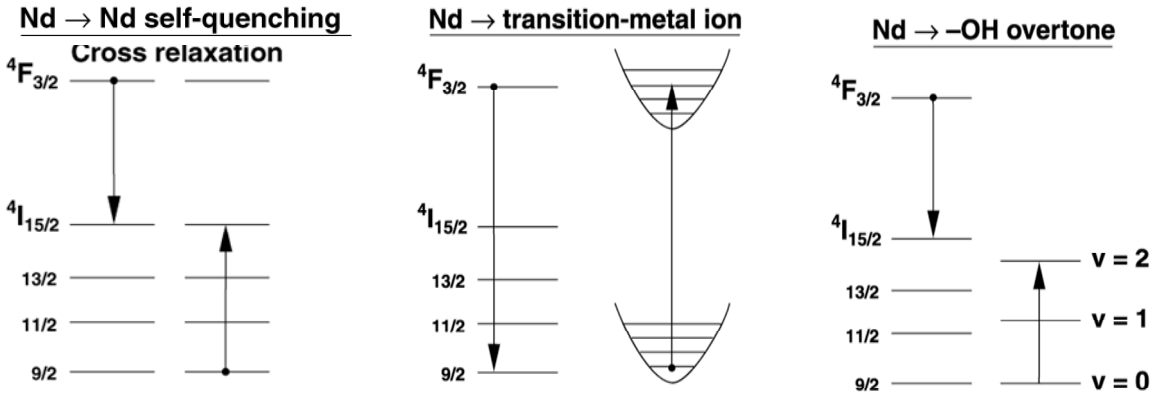


Figure 10. Schematic representation of major mechanisms for non-radiative energy loss from the $^4F_{3/2}$ state (i.e. upper laser level): (a) Nd-to-Nd energy transfer (self-quenching), (b) energy transfer to OH vibrational modes and (c) transition metal vibronic excitations.

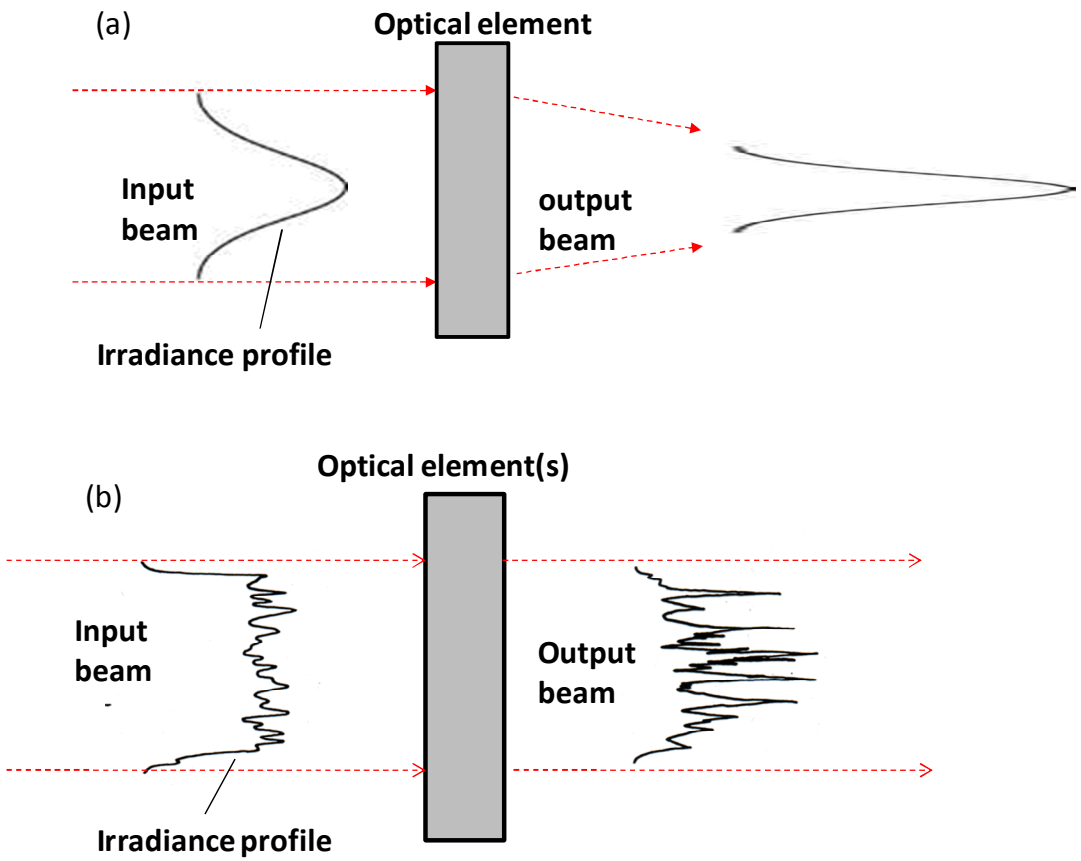


Figure 11. Illustration of (a) whole beam and (b) localized self-focusing during propagation of a high intensity laser beam through an optical material of refractive index n(I).

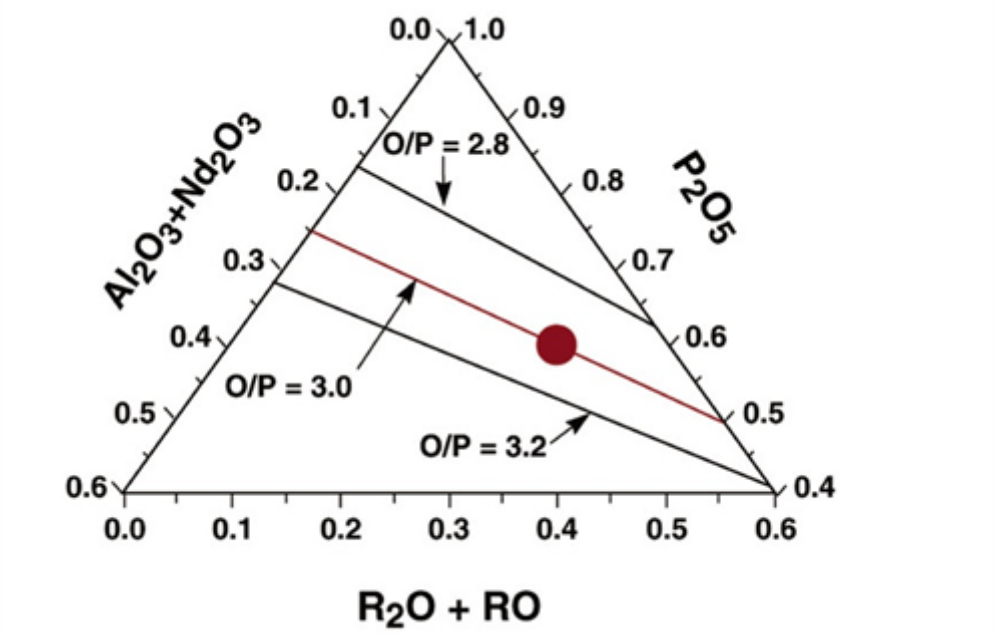


Figure 12. Ternary composition diagram for the $P_2O_5$-$Al_2O_3$/$RE_2O_3$-MO/$M_2O$ system showing the approximate compositional region (as indicated by the spot) for most commercial HEHP and HAP laser glasses. These glasses have an O/P ratio of about 3/1 (i.e. "meta-phosphate") implying a backbone structure of rings and long chains of $PO_3$ groups. The units of the plot are in mole fraction.

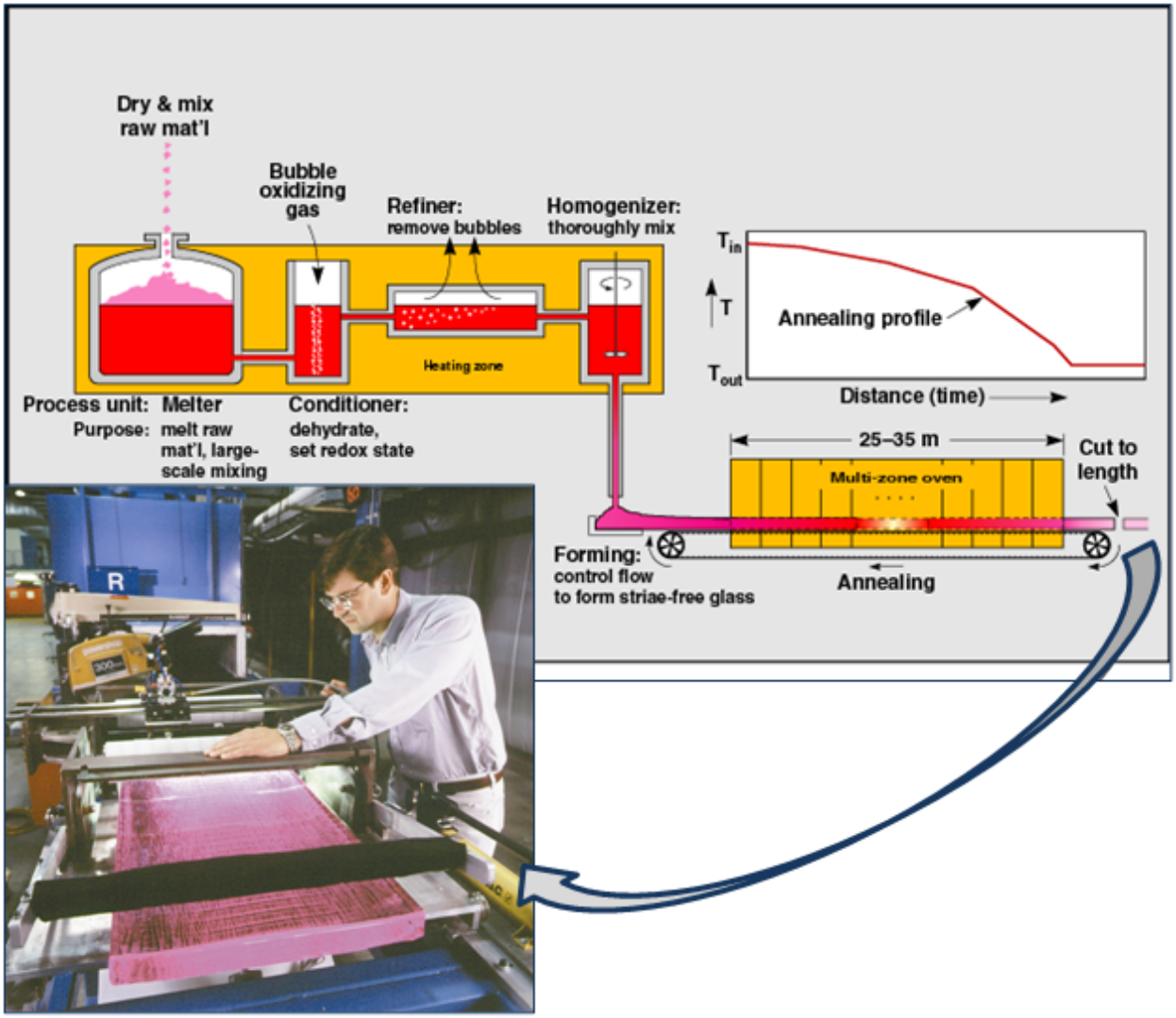


Fig. 13. Schematic representation of the continuous melting process used to prepare HEHP laser glass blanks from which finished laser slabs are fabricated.

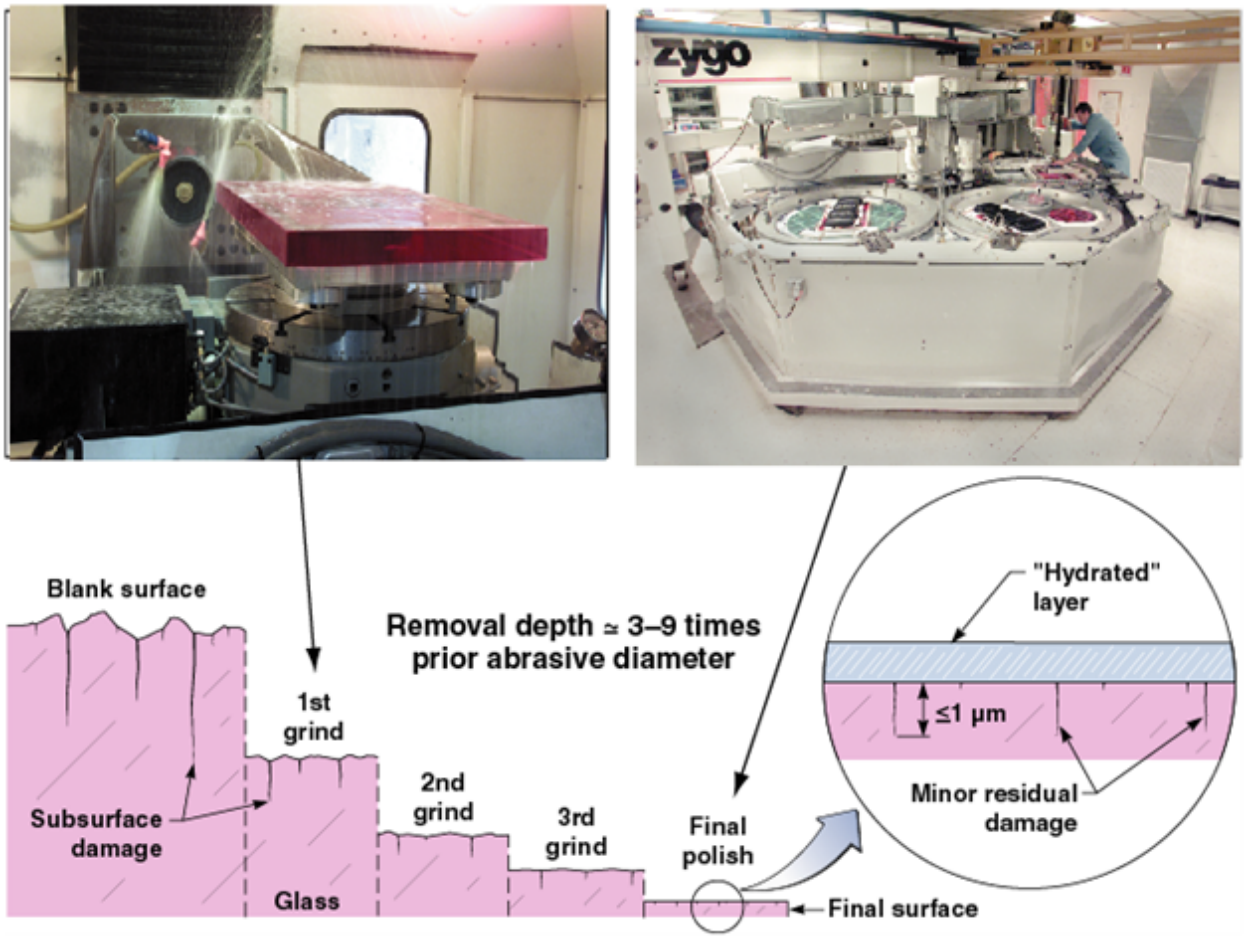


Fig. 14. Optical "finishing" uses a combination of grinding and polishing steps that successively remove material from the glass surface in incrementally smaller amounts. The goal is to remove sufficient material to eliminate all subsurface fractures (defects) produced by the previous step. The subsurface damage is generally less than 1um deep and widely dispersed at completion of the final precision polishing step.